Global fit to the 2HDM with generic sources of flavour violation using GAMBIT

Peter Athron ⓘ,[a] **Andreas Crivellin** ⓘ,[b,c] **Tomás E. Gonzalo** ⓘ,[d] **Syuhei Iguro** ⓘ[e,f,g] **and Cristian Sierra** ⓘ[a]

[a]*Department of Physics and Institute of Theoretical Physics, Nanjing Normal University,*
 Wenyuan Road, Nanjing, Jiangsu, 210023, China
[b]*Physik-Institut, Universität Zürich,*
 Winterthurerstrasse 190, CH–8057 Zürich, Switzerland
[c]*PSI Center for Neutron and Muon Sciences,*
 5232 Villigen PSI, Switzerland
[d]*Institut für Theoretische Teilchenphysik, Karlsruher Institut für Technologie (KIT),*
 D-76128 Karlsruhe, Germany
[e]*Institute for Advanced Research (IAR), Nagoya University,*
 Nagoya 464–8601, Japan
[f]*Kobayashi-Maskawa Institute (KMI) for the Origin of Particles and the Universe,*
 Nagoya University,
 Nagoya 464–8602, Japan
[g]*KEK Theory Center, IPNS, KEK,*
 Tsukuba 305–0801, Japan
 E-mail: peter.athron@coepp.org.au, andreas.crivellin@psi.ch,
 tomas.gonzalo@kit.edu, igurosyuhei@gmail.com,
 cristian.sierra@njnu.edu.cn

ABSTRACT: We perform a global statistical analysis of the two-Higgs-doublet model with generic sources of flavour violation using GAMBIT. This is particularly interesting in light of deviations from the Standard Model predictions observed in $b \to c\tau\bar{\nu}$ and $b \to s\ell^+\ell^-$ transitions as well as the indications for a charged Higgs with a mass of $130\,\mathrm{GeV}$ in top quark decays. Including all relevant constraints from precision, flavour and collider observables, we find that it is possible to simultaneously explain both the charged and neutral current B anomalies. We study the impact of using different values for the W mass and the Standard Model prediction for the anomalous magnetic moment of the muon and provide predictions for observables that can probe our model in the future such as lepton flavour violation searches at Belle II and Higgs coupling strength measurements at the high-luminosity LHC.

Contents

1 Introduction

The Standard Model (SM) is extremely successful in describing the interactions of matter at sub-atomic scales [1]. However, several intriguing deviations from the SM predictions of more than 3 standard deviations, called anomalies, exist [2]. In particular, the long-standing anomalies in semi-leptonic B meson decays [3], both in $b \to c\tau\overline{\nu}$ [4] transitions, i.e. $R(D)$ and $R(D^*)$, (3.3σ) and in $b \to s\ell^+\ell^-$ observables $(\approx 6\sigma)$ persist; see ref. [5] for an overview. These observables point towards new physics (NP) and motivate the study of models capable of providing a combined explanation. Furthermore, there is a 3σ excess in the exotic top decay $t \to b(H^+ \to \bar{b}c)$ [6] which motivates an extension of the scalar sector.

In this article, we investigate the possibility of a NP explanation of these anomalies within the context of the two-Higgs-doublet model (2HDM) [7, 8] — one of the simplest and most studied extensions of the SM scalar sector. The most general version with generic Yukawa couplings (G2HDM)[1] can explain $b \to c\tau\nu$ data at the 1σ level [9–24] and address the anomalies in $b \to s\ell^+\ell^-$ transitions [24–28], even though reaching the preferred central value of the latter is difficult. To evade constraints from collider searches, $B_s - \bar{B}_s$ mixing etc,

---

[1]Sometimes this is also referred to as the type III 2HDM in the literature.

only quite small regions of the parameter space remain valid and only particular benchmark points have been examined, while a combined statistical analysis of all available data and an identification of the allowed parameter space is still missing.[2] Furthermore, contributions to other precision observables such as the anomalous magnetic moment of the muon $((g-2)_\mu)$ and the mass of the W boson (m_W) are in general expected in 2HDMs and have to be included in a global statistical analysis, even though the experimental and theoretical situation is not conclusive in these cases, as we will discuss in detail later.

Such a global statistical analysis is the aim of this article. For this, we extend the work of refs. [18, 24] by including, for instance, recent measurements of the charged lepton flavour violating (cLFV) search in $t \to \mu\tau q$ decays from ATLAS [30] and the latest flavour universality test update from Belle II on the ratio between the muon and electron couplings to the W boson $(|g_\mu/g_e|)$ [31]. In addition to extending the set of observables and updating the data, we allow for additional Yukawa couplings to be non-zero which were previously not studied. For instance, an additional charm quark Yukawa coupling could enhance the effect in $b \to s\ell^+\ell^-$ [24]. We perform this global fit using the inference package GAMBIT, the Global And Modular Beyond-the-Standard-Model Inference Tool [32, 33], which is an open-source code in C++ to calculate observables and likelihoods for generic beyond the Standard Model (BSM) theories utilising different modules and external packages (see section 4 for more details).

The paper is organised as follows: in section 2 we introduce the G2HDM model and in section 3 we list the relevant observables, including flavour, collider and precision observables and afterwards present the results of the global fit and predictions for future experiments in section 4. Finally, we conclude in section 5 and show the potential impact of a sizeable NP effect in $g-2$ of the muon on the fit in the appendix.

2 The general two Higgs doublet model

The most general renormalisable scalar potential respecting gauge invariance is [7, 8]

$$
\begin{aligned}
V(\Phi_1, \Phi_2) = {} & m_{11}^2(\Phi_1^\dagger \Phi_1) + m_{22}^2(\Phi_2^\dagger \Phi_2) - m_{12}^2(\Phi_1^\dagger \Phi_2 + \Phi_2^\dagger \Phi_1) \\
& + \frac{1}{2}\lambda_1(\Phi_1^\dagger \Phi_1)^2 + \frac{1}{2}\lambda_2(\Phi_2^\dagger \Phi_2)^2 + \lambda_3(\Phi_1^\dagger \Phi_1)(\Phi_2^\dagger \Phi_2) + \lambda_4(\Phi_1^\dagger \Phi_2)(\Phi_2^\dagger \Phi_1) \\
& + \left(\frac{1}{2}\lambda_5(\Phi_1^\dagger \Phi_2)^2 + \left(\lambda_6(\Phi_1^\dagger \Phi_1) + \lambda_7(\Phi_2^\dagger \Phi_2)\right)(\Phi_1^\dagger \Phi_2) + \text{ h.c.} \right),
\end{aligned}
\tag{2.1}
$$

where the parameters m_{11}^2, m_{22}^2 and λ_{1-4} are real numbers (from hermiticity), whereas the $\lambda_{5,6,7}$ and m_{12}^2 can in general be complex. For a CP-conserving potential, which we assume in the following, all parameters in eq. (2.1) are real and the total number of free parameters will be reduced from 14 to 10. Note that in our discussion of the flavour observables, only the resulting mixing angles among the scalars and their masses are relevant. We will come back to this point at the beginning of section 2.1.

Once the two scalars develop non-zero vacuum expectation values (VEVs) v_1 and v_2, the electroweak symmetry of the SM is spontaneously broken and the doublets are decomposed

---

[2]Efforts in this direction have been presented in the quark [29] and lepton sectors [18], separately.

into components as

$$\Phi_i = \begin{pmatrix} \phi_i^+ \\ \frac{1}{\sqrt{2}}(v_i + \rho_i + i\eta_i) \end{pmatrix}, \quad i = 1, 2. \tag{2.2}$$

Linear combinations of the fields ρ_i, η_i and $\phi_i^\pm$ form mass eigenstates

$$\begin{pmatrix} G_Z \\ A \end{pmatrix} = R_\beta \begin{pmatrix} \eta_1 \\ \eta_2 \end{pmatrix}, \quad \begin{pmatrix} G_{W^\pm} \\ H^\pm \end{pmatrix} = R_\beta \begin{pmatrix} \phi_1^\pm \\ \phi_2^\pm \end{pmatrix}, \quad \begin{pmatrix} H \\ h \end{pmatrix} = R_\alpha \begin{pmatrix} \rho_1 \\ \rho_2 \end{pmatrix}, \tag{2.3}$$

where ϕ_i^+ are electrically charged complex scalars and η_i and ρ_i neutral real scalars. $G_{W^\pm}$ and G_Z correspond to longitudinal components of the W and Z bosons, while h (the SM-like Higgs) and H are physical CP-even states, A a CP-odd state and $H^\pm$ is a charged Higgs boson. The rotation matrices are defined as

$$R_\theta = \begin{pmatrix} \cos\theta & \sin\theta \\ -\sin\theta & \cos\theta \end{pmatrix}, \tag{2.4}$$

where θ is either α or β. The angle α is the mixing angle of the CP-even states, whereas the rotation angle β is determined by

$$\tan\beta \equiv t_\beta = \frac{s_\beta}{c_\beta} = \frac{v_2}{v_1}, \tag{2.5}$$

with $\{s_\beta, c_\beta\} = \{\sin\beta, \cos\beta\}$ and $v_2^2 + v_1^2 = v^2$ with $v = 246\,\text{GeV}$ being the SM VEV. The angle defined by $\beta - \alpha$ is the mixing angle between the CP-even Higgs mass eigenstates relative to the Higgs basis and the limit $\sin(\beta - \alpha) \equiv s_{\beta\alpha} \to 1$ is known as the alignment limit in which h has the same properties as the SM Higgs.

The most general Yukawa Lagrangian in the basis $\{\Phi_1, \Phi_2\}$ reads [8]

$$-\mathcal{L}_{\text{Yukawa}} = \bar{Q}^0 (Y_u^1 \tilde{\Phi}_1 + Y_u^2 \tilde{\Phi}_2) u_{\text{R}}^0 + \bar{Q}^0 (Y_d^1 \Phi_1 + Y_d^2 \Phi_2) d_{\text{R}}^0 + \bar{L}^0 (Y_l^1 \Phi_1 + Y_l^2 \Phi_2) l_{\text{R}}^0 + \text{ h.c.}, \tag{2.6}$$

where the superscript "0" notation refers to the flavour eigenstates, and $\tilde{\Phi}_j = i\sigma_2 \Phi_j^*$. The fermion mass matrices are determined by

$$M_f = \frac{1}{\sqrt{2}}(v_1 Y_f^1 + v_2 Y_f^2), \qquad f = u, d, l, \tag{2.7}$$

and are in general non-diagonal. Via a bi-unitary transformation

$$\bar{M}_f = V_{fL}^\dagger M_f V_{fR}, \tag{2.8}$$

the mass eigenstates for the fermions are given by

$$u = V_u^\dagger u^0, \qquad d = V_d^\dagger d^0, \qquad l = V_l^\dagger l^0, \tag{2.9}$$

with

$$\bar{M}_f = \frac{1}{\sqrt{2}}(v_1 \tilde{Y}_f^1 + v_2 \tilde{Y}_f^2), \tag{2.10}$$

where $\tilde{Y}_f^i = V_{fL}^\dagger Y_f^i V_{fR}$. We shall drop the tilde from now on. Solving for Y_f^1 we have

$$Y_f^{1,ba} = \frac{\sqrt{2}}{v \cos \beta} \bar{M}_f^{ba} - \tan \beta \, Y_f^{2,ba}, \tag{2.11}$$

and can write the Yukawa Lagrangian in the mass basis as

$$-\mathcal{L}_{\text{Yukawa}} = \bar{u}_b \left(V_{bc} \rho_d^{ca} P_R - V_{ca} \rho_u^{cb*} P_L \right) d_a \, H^+ + \bar{\nu}_b \rho_\ell^{ba} P_R l_a \, H^+ + \text{h.c.} \\ + \sum_{f=u,d,\ell} \sum_{\phi=h,H,A} \bar{f}_b \, \Gamma_f^{\phi ba} P_R f_a \phi + \text{h.c.}, \tag{2.12}$$

where $a, b, c = 1, 2, 3$,

$$\rho_f^{ba} \equiv \frac{Y_f^{2,ba}}{\cos \beta} - \frac{\sqrt{2} \tan \beta \, \bar{M}_f^{ba}}{v}, \tag{2.13}$$

$$\Gamma_f^{hba} \equiv \frac{\bar{M}_f^{ba}}{v} s_{\beta\alpha} + \frac{1}{\sqrt{2}} \rho_f^{ba} c_{\beta\alpha}, \tag{2.14}$$

$$\Gamma_f^{Hba} \equiv \frac{\bar{M}_f^{ba}}{v} c_{\beta\alpha} - \frac{1}{\sqrt{2}} \rho_f^{ba} s_{\beta\alpha}, \tag{2.15}$$

$$\Gamma_f^{Aba} \equiv \begin{cases} -\dfrac{i}{\sqrt{2}} \rho_f^{ba} & \text{if } f = u, \\ \dfrac{i}{\sqrt{2}} \rho_f^{ba} & \text{if } f = d, \ell \,, \end{cases} \tag{2.16}$$

and $s_{\beta\alpha} \equiv \sin(\beta - \alpha)$, $c_{\beta\alpha} \equiv \cos(\beta - \alpha)$. Later when evaluating the indices in eq. (2.13) for the specific lepton or Yukawa sectors we will switch to the respective flavour notation.

2.1 Model parameters

Note that the B anomalies are related to second and third generation quarks and leptons. Therefore, we do not consider extra Yukawa couplings involving interactions with the first generation. More specifically, we parametrise the Yukawa matrices as[3]

$$\rho_u = \begin{pmatrix} 0 & 0 & 0 \\ 0 & \rho_u^{cc} & 0 \\ 0 & \rho_u^{tc} & \rho_u^{tt} \end{pmatrix}, \qquad \rho_d = \begin{pmatrix} 0 & 0 & 0 \\ 0 & 0 & 0 \\ 0 & 0 & \rho_d^{bb} \end{pmatrix}, \qquad \rho_\ell = \begin{pmatrix} 0 & 0 & \rho_\ell^{e\tau} \\ 0 & \rho_\ell^{\mu\mu} & \rho_\ell^{\mu\tau} \\ 0 & 0 & \rho_\ell^{\tau\tau} \end{pmatrix}, \tag{2.17}$$

where we have extended the pattern of ref. [24] to include the second generation diagonal Yukawas for both the lepton and up-type matrices, $\rho_\ell^{\mu\mu}$ and ρ_u^{cc} as well as third generation down-type quark coupling ρ_d^{bb}. The diagonal down-type Yukawa coupling ρ_d^{ss} (ρ_u^{ct}) is however ignored because of strong constraints from the LHC ($b \to s\gamma$), and we choose to consider $\rho_\ell^{\mu\tau,e\tau}$ but not $\rho_\ell^{\tau\mu,\tau e}$ because the simultaneous effect would lead to chirally enhanced effects in $\mu \to e\gamma$ and $\tau \to \mu\gamma, e\gamma$ [10, 34]. Furthermore, the (effective) Yukawa couplings ρ_f^{ba} are derived from the Yukawa couplings $Y_f^{2,ba}$ via the transformation in eq. (2.13), with an

---

[3]Here we use flavour indices, so c stands for charm and b stands for bottom, rather than being indices that run over the generations.

explicit dependence on $\tan\beta$. Hence, to avoid this explicit dependence on $\tan\beta$ on the model parameters, we will use as fundamental scan parameters the extra Yukawas $Y_f^{2,ba}$, which corresponds to work in the Higgs basis, i.e. NP Yukawa interactions will be encoded only in the $Y_f^{2,ba}$ parameters.

Concerning the scalar potential, we switch from $\lambda_1 - \lambda_5$ the parameters to the mass-like parameters m_h, m_H, m_A, $m_{H^\pm}$ and m_{12}. Furthermore, the effect of λ_6 and λ_7 of electroweak (EW) precision data and flavour observables is automatically included (at the one-loop level). Therefore, the only parameters of the scalar sector are m_H, m_A, $m_{H^\pm}$, m_{12}, $\tan\beta$ and $s_{\beta\alpha}$.

We used the following ranges for the parameters, based on the findings of ref. [10]

$$m_{12} \in [-200, 200]\,\mathrm{GeV}, \qquad m_{H^\pm} \in [120, 140]\,\mathrm{GeV}, \qquad m_A,\, m_H \in [150, 350]\,\mathrm{GeV},$$

$$s_{\beta\alpha} \in [0.98, 1.0], \qquad \tan\beta \in [0.01, 10], \qquad Y_u^{2,tt} \in [-1.0, 1.0], \qquad Y_u^{2,tc} \in [-0.6, 0.6],$$

$$\mathrm{Re},\, \mathrm{Im}(Y_\ell^{2,\tau\tau}) \in [-0.1, 0.1], \qquad Y_\ell^{2,e\tau},\, Y_\ell^{2,\mu\tau} \in [-0.01, 0.01],$$

$$Y_u^{2,cc} \in [-0.15, 0.15], \qquad Y_d^{2,bb} \in [-0.2, 0.2], \qquad Y_\ell^{2,\mu\mu} \in [-0.1, 0.1]. \tag{2.18}$$

Note that we allow for a complex $Y_\ell^{2,\tau\tau}$ to explain the $b \to c\tau\nu$ anomaly while other couplings are taken to be real. We work close to the alignment limit, i.e. $s_{\beta\alpha} \in [0.98, 1.0]$ such that the bounds from SM Higgs signal strength are satisfied.[4]

3 Observables

The flavour-violating couplings of the G2HDM enter in many different processes. Here we present the observables relevant to our analysis and give the corresponding NP contributions.

3.1 Top decays

The ATLAS collaboration reported an excess in $t \to bH^+ \to b\bar{b}c$ [6]

$$\mathrm{BR}(t \to bH^+ \to b\bar{b}c) = (0.16 \pm 0.06)\% \tag{3.1}$$

for a charged Higgs mass of $m_{H^\pm} = 130\,\mathrm{GeV}$, which corresponds to a global (local) significance of $2.5\,(3.0)\sigma$. Then the corresponding G2HDM contribution to the decay is given as

$$\mathrm{BR}(t \to bH^+ \to b\bar{b}c) \approx \frac{m_t(|\rho_u^{tt}|^2 + |\rho_d^{bb}|^2)}{16\pi\Gamma_t}\left(1 - \frac{m_{H^\pm}^2}{m_t^2}\right)^2 \frac{3|\rho_u^{tc}|^2}{3|\rho_u^{tc}|^2 + 3|\rho_u^{cc}|^2 + \sum_{l,l'}|\rho_\ell^{ll'}|^2}, \tag{3.2}$$

where Γ_t is the total decay width of the top quark.

For the lepton flavour violating decay $t \to \mu\tau q$ [30] an upper bound of

$$\mathrm{BR}(t \to \mu^+\tau^-c) < (8.2 \pm 0.5) \times 10^{-7}, \tag{3.3}$$

at the 90% CL is found. In the G2HDM the corresponding width is given by

$$\Gamma(t \to \mu^+\tau^-c) = \frac{m_t^5}{3072\,\pi^3}\left|c_{\mathrm{lequ}}^{1(\mu\tau ct)}\right|^2, \tag{3.4}$$

---

[4]We consider here only the bounds from fermionic decays of the Higgs since the di-photon signal strength can always be brought into agreement with the measurement by choosing an appropriate value of λ_7 [35].

with

$$c_{\text{lequ}}^{1(\mu\tau ct)} = \frac{\rho_u^{tc*}\rho_\ell^{\mu\tau}}{2}\left(\frac{c_{\beta-\alpha}^2}{m_h^2} + \frac{s_{\beta-\alpha}^2}{m_H^2} + \frac{1}{m_A^2}\right). \tag{3.5}$$

Note that the quark in the final state is only a charm quark given that we are ignoring couplings to first generation quarks.[5]

For the decay of a top quark to a charm quark and the SM Higgs, we have in the G2HDM [24]

$$\text{BR}(t \to hc) = \frac{m_t c_{\beta\alpha}^2 |\rho_u^{tc}|^2}{64\pi\Gamma_t}\left(1 - \frac{m_h^2}{m_t^2}\right)^2 \approx 2.4 \times 10^{-4}\left(\frac{\rho_u^{tc}c_{\beta\alpha}}{0.05}\right)^2, \tag{3.6}$$

which can be compared to the current ATLAS [37] (CMS [38]) upper limit $\text{BR}(t \to hc) \leq 4.0 \times 10^{-4}$ (3.5×10^{-4}).

3.2 Charged current anomalies in $b \to c\ell\bar{\nu}$

The ratios

$$R(D^{(*)}) = \frac{\text{BR}(\bar{B} \to D^{(*)}\tau\bar{\nu})}{\text{BR}(\bar{B} \to D^{(*)}l\bar{\nu})}, \tag{3.7}$$

with $l = e, \mu$, have been measured by LHCb [39–41], Belle [42–45], Belle-II [46] and BaBar [47, 48]. The combination provided by HFLAV [49] is

$$R(D)_{\text{HFLAV}} = 0.342 \pm 0.026, \quad R(D^*)_{\text{HFLAV}} = 0.287 \pm 0.012. \tag{3.8}$$

Using the form factors [50, 51] provided in Superlso 4.1 [52–54], the G2HDM contributions to $R(D)$ and $R(D^*)$ are given by

$$R(D) \approx \frac{1 + 1.73\,\text{Re}(g_S^{\tau\tau}) + 1.35\sum\left|g_S^{l\tau}\right|^2}{3.27 + 0.57\,\text{Re}(g_S^{\mu\mu}) + 4.8\sum|g_S^{l\mu}|^2}, \qquad R(D^*) \approx \frac{1 + 0.11\,\text{Re}(g_P^{\tau\tau}) + 0.04\sum\left|g_P^{l\tau}\right|^2}{4.04 + 0.08\,\text{Re}(g_P^{\mu\mu}) + 0.25\sum|g_P^{l\mu}|^2}, \tag{3.9}$$

with $l = e, \mu, \tau$ and $R(D)_{\text{SM}} = 0.306$ and $R(D^*)_{\text{SM}} = 0.247$. The scalar and pseudoscalar couplings $g_{S,P}^{ll'}$ are given in the G2HDM as [18],

$$g_S^{ll'} \equiv \frac{C_R^{cb} + C_L^{cb}}{C_{SM}^{cb}}, \qquad g_P^{ll'} \equiv \frac{C_R^{cb} - C_L^{cb}}{C_{SM}^{cb}}, \tag{3.10}$$

where $C_{SM}^{cb} = 4G_F V_{cb}/\sqrt{2}$ and

$$C_R^{cb} = -\frac{(V_{cb}\rho_d^{bb} + V_{cs}\rho_d^{sb})\rho_\ell^{ll'*}}{m_{H^\pm}^2}, \qquad C_L^{cb} = \frac{(V_{tb}\rho_u^{tc*} + V_{cb}\rho_u^{cc*})\rho_\ell^{ll'*}}{m_{H^\pm}^2}, \tag{3.11}$$

which includes the renormalisation group correction factor of 1.5 [55–58] as a multiplicative factor in the Wilson coefficients (WCs) of eq. (3.11).

---

[5]ATLAS [36] recently searched for $H^+ \to c\bar{s}$ reporting no significant excess. However, in our current setup, we have $\text{BR}(H^+ \to c\bar{s}) < \text{BR}(H^+ \to c\bar{b})$ and the mis-tagging rate of a strange quark as a b quark is small, such that one can evade this constraint.

In addition to $R(D^{(*)})$, the Belle experiment also measured the lepton flavour universality (LFU) ratio $R_{e/\mu} = \mathrm{BR}(\bar{B} \to De\bar{\nu})/\mathrm{BR}(\bar{B} \to D\mu\bar{\nu})$ to be [59]

$$R_{e/\mu} = 1.01 \pm 0.01 \pm 0.03, \tag{3.12}$$

which can be expressed in the G2HDM as [18]

$$R_{e/\mu} \approx \frac{1}{0.9964 + 0.18 \, \mathrm{Re}[g_S^{\mu\mu}] + 1.46 \sum_l \left| g_S^{l\mu} \right|^2}, \tag{3.13}$$

where we have obtained the NP leptonic contributions by integrating the heavy quark effective theory amplitudes of the scalar type operators from refs. [60, 61].

3.3 Leptonic meson decays

The fully leptonic decays of mesons can receive chirally enhanced effects from (pseudo-) scalar currents compared to the SM vector currents. The total decay width in the G2HDM is [14, 62, 63]

$$\mathrm{BR}(M_{ij} \to l\nu) = G_F^2 m_l^2 f_M^2 \tau_M |V_{ij}|^2 \frac{m_M}{8\pi} \left(1 - \frac{m_l^2}{m_M^2} \right)^2 \left[|1 - \Delta_{ij}^{ll}|^2 + |\Delta_{ij}^{l'l}|^2 \right], \tag{3.14}$$

where i, j are the valence quarks of the meson M, f_M is its decay constant and $\Delta_{ij}^{ll'}$ is the NP correction given by

$$\Delta_{ij}^{l'l} = \left(\frac{m_M}{m_{H^\pm}} \right)^2 Z_{l'l}^* \left(\frac{Y_{ij} m_{u_i} + X_{ij} m_{d_j}}{V_{ij}(m_{u_i} + m_{d_j})} \right), \quad l \neq l', \ \ l,l' = 2,3, \tag{3.15}$$

with

$$X_{ij} = \frac{v}{\sqrt{2}m_{d_j}} V_{ik} \rho_d^{kj}, \qquad Y_{ij} = \frac{v}{\sqrt{2}m_{u_i}} \rho_u^{ki*} V_{kj}, \qquad Z_{l'l} = \frac{v}{\sqrt{2}m_j} \rho_\ell^{l'l}. \tag{3.16}$$

In particular, we consider the experimental measurements from HFLAV [49] $\mathrm{BR}(D_s \to \mu\bar{\nu}) = (5.43 \pm 0.15) \times 10^{-3}$, $\mathrm{BR}(D_s \to \tau\bar{\nu}) = (5.32 \pm 0.11) \times 10^{-2}$ and $\mathrm{BR}(B_c \to \tau\bar{\nu})$. Regarding the latter, the theoretical prediction within the SM is still unclear and upper limits of 60% [64–66] are still possible. To be conservative, we define a likelihood function allowing values for $\mathrm{BR}(B_c \to \tau\bar{\nu}) \leq 70\%$. The expression for the SM plus the G2HDM contribution for $\mathrm{BR}(B_c \to \tau\bar{\nu})$ is given at tree level [67] as,

$$\mathrm{BR}(B_c \to \tau\bar{\nu}) \approx \mathrm{BR}(B_c \to \tau\bar{\nu})_{\mathrm{SM}} \left[|1 - 4.35 \, C_L^{\tau\tau}|^2 + 4.35^2 \left(|C_L^{e\tau}|^2 + |C_L^{\mu\tau}|^2 \right) \right]. \tag{3.17}$$

3.4 Neutral current anomalies: $b \to s$ transitions

Global fits to $b \to s\ell^+\ell^-$ observables favour a vectorial coupling $C_9^U \approx -1$ at the 5σ level [3, 5, 68–73], where the U stands for lepton universal. The most relevant observables include the so-called P_5' [74–77],[6] the total branching ratio and angular observables in

---

[6]Recently, the CMS collaboration [78] made competitive measurements of the angular observables in good agreement with LHCb data confirming the anomaly. For more details and complete expressions for the angular observables the reader is referred to refs. [18, 79, 80].

$B_s \to \phi\,\mu^+\mu^-$ [81–83] as well as the BR$(B \to K\mu^+\mu^-)$ [84–86], which are fully compatible with semi-inclusive observables [87], i.e., those obtained from the sum of the leading exclusive modes. This inspires lepton flavour universal NP models with vectorial couplings to leptons and left-handed couplings to bottom and strange quarks that may relax the tension.

In the G2HDM model, mainly the charm loop contributes to C_9^U via an off-shell photon penguin [25–28, 88–90] and we obtain [26],

$$\Delta C_9^U(\mu_b) \approx -0.52 \left(\frac{|\rho_u^{tc}|^2 - |\rho_u^{cc}|^2}{0.5^2} \right) + 0.50 \left(\frac{\rho_u^{tc*}\rho_u^{cc}}{0.01} \right), \tag{3.18}$$

for $m_{H^\pm} = 130$, although later we use the full logarithmic dependence with $m_{H^\pm}$ in our global fit. We see that a sizeable coupling ρ_u^{tc} is necessary if $\rho_u^{cc} \approx 0$ is assumed while the product $\rho_u^{tc*}\rho_u^{cc}$ has a Cabibbo-Kobayashi-Maskawa (CKM) enhancement w.r.t. the SM. While in the previous work [24] the value of ρ_u^{cc} was set to zero, it could play an important role in obtaining values in agreement with model-independent fits. In addition to the contributions to C_9^U, the closely-related quark level decay $b \to c\bar{c}s$ can noticeably affect the B_s meson lifetime [88, 91] and potentially constrain the G2HDM. Since it is not easy to control the exclusive decay $b \to c\bar{c}s$, the lifetime ratio τ_{B_s}/τ_{B_d} is typically used, which can be calculated with a heavy bottom quark expansion. Nevertheless, in our scenario thanks to the CKM suppressed $b \to c\bar{c}d$ interaction this shift in the ratio is cancelled, significantly relaxing the constraint and hence we will not consider it henceforth.

Regarding scalar operators with coefficients $C_{Q_{1,2}}$, which are also present in the effective Hamiltonian describing $b \to s\ell^+\ell^-$ observables, the most sensitive observable is the branching ratio BR$(B_s \to \mu^+\mu^-)$ which also depends on the coupling $C_{10}^{(\prime)} = C_{10}^{(\prime)\mathrm{SM}} + \Delta C_{10}^{(\prime)}$ related to the pseudo-vector operator [80],

$$\mathrm{BR}(B_s \to \mu^+\mu^-) = \frac{G_F^2 \alpha^2}{64\pi^3} f_{B_s}^2 \tau_{B_s} m_{B_s}^3 \left| V_{tb}V_{ts}^* \right|^2 \sqrt{1 - \frac{4m_\mu^2}{m_{B_s}^2}}$$
$$\times \left[\left(1 - \frac{4m_\mu^2}{m_{B_s}^2} \right) \left| \frac{m_{B_s}\left(C_{Q_1} - C_{Q_1}' \right)}{(m_b + m_s)} \right|^2 + \left| \frac{m_{B_s}\left(C_{Q_2} - C_{Q_2}' \right)}{(m_b + m_s)} - 2\left(C_{10} - C_{10}' \right) \frac{m_\mu}{m_{B_s}} \right|^2 \right], \tag{3.19}$$

where f_{B_s} is the B_s meson decay constant, τ_{B_s} is its mean lifetime and the WCs in the G2HDM are given in refs. [18, 26]. The experimental data for all these observables are taken from the HEPLike package [92], whereas the theoretical predictions are extracted from SuperIso [52–54].

For the radiative inclusive decay $\bar{B} \to X_s\gamma$, the contributions from the G2HDM are taken from refs. [93–98] as implemented in SuperIso [52–54]. As a function of the C_7 and C_7' Wilson coefficients related to the electromagnetic operators, the $b \to s\gamma$ transition rate can be written as

$$\Gamma(b \to s\gamma) = \frac{G_F^2}{32\pi^4} |V_{tb}V_{ts}^*|^2 \alpha_{\mathrm{em}}\, m_b^5 \left(|C_{7\mathrm{eff}}(\mu_b)|^2 + |C_{7\mathrm{eff}}'(\mu_b)|^2 \right), \tag{3.20}$$

where $C_{7\mathrm{eff}}^{(\prime)} = C_{7\mathrm{eff}}^{(\prime)\mathrm{SM}} + \Delta C_{7\mathrm{eff}}^{(\prime)}$ is the effective WC (see below), and the experimental measurement is BR$(B \to X_s\gamma) \times 10^4 = 3.49 \pm 0.19$ [4]. Taking into account the $1/\sqrt{2}$ factor

difference in the notations with respect to ref. [26], the dominant top quark contribution for the ΔC_7 WC is given by

$$\Delta C_7^{t, H^\pm} = -\frac{1}{36} \frac{m_W^2}{m_{H^\pm}^2} \frac{V_{ks}^* \rho_u^{kt} \rho_u^{nt*} V_{nb}}{g_2^2 V_{tb} V_{ts}^*} f_1 \left(\frac{m_t^2}{m_{H^\pm}^2} \right), \tag{3.21}$$

where $f_1(x)$ is a loop function one can find in ref. [26] from where again we use all expressions for computing the WCs. While the charm quark contribution is obtained as,

$$\Delta C_7^{c, H^\pm}(\mu) = -\frac{7}{36} \frac{m_W^2}{m_{H^\pm}^2} \frac{V_{ks}^* \rho_u^{kc} \rho_u^{nc*} V_{nb}}{g_2^2 V_{tb} V_{ts}^*}. \tag{3.22}$$

Numerically with $m_{H^\pm} = 130\,\text{GeV}$ one gets

$$\Delta C_{7\text{eff}}(\mu_b) \approx -0.174 \left(|\rho_u^{tc}| \right)^2 - 0.046 \left(|\rho_u^{tt}| \right)^2, \tag{3.23}$$

which can be used for understanding possible explanations of the anomaly in $t \to bH^+ \to b\bar{b}c$. We note that C_7 of the SM is negative which fixes the convention and hence $\Delta C_{7\text{eff}}$ constructively interferes with the SM contribution. Furthermore, we have implemented the respective RGE effects in GAMBIT including the mixing with the C_8 WC that is the one associated with the chromomagnetic operator. From model independent fits, we require the NP contribution to be within $-0.04 \leq \Delta C_7(\mu_b) \leq 0.04$ [5]. Additionally, once we turn on the second-generation diagonal quark Yukawas we will have mixed terms given by the semi-numerical expression

$$\Delta C_{7\text{eff}}^{\text{mix}}(\mu_b) \approx 0.105 \left(\frac{\rho_u^{tc*} \rho_u^{cc}}{0.025} \right) - 0.028 \left(\frac{\rho_u^{cc} \rho_d^{bb}}{0.025} \right) + 0.19 \left(\frac{\rho_u^{tt*} \rho_d^{bb}}{0.025} \right), \tag{3.24}$$

where again we have fixed $m_{H^\pm} = 130\,\text{GeV}$. We note that these terms can take both signs depending on the sign of the coupling product and hence potentially cancel the negative contribution from eq. (3.23).

Last, the recent measurement of $\text{BR}(B^+ \to K^+ \nu\bar{\nu})$ by Belle II is yet another exciting hint of NP [99]. Given its close relation to the $b \to s\ell^+\ell^-$ decays one could expect both a Z penguin and box diagram contribution enhancement in the G2HDM. However, the necessary WCs turn out to be very suppressed by all other flavour constraints at the 2σ level, implying an SM-like prediction for $\text{BR}(B^+ \to K^+ \nu\bar{\nu})$.

3.5 $B_s - \overline{B_s}$ mixing

The mass difference of the B_s and $\overline{B_s}$ mesons in the presence of NP is commonly written as [100]

$$\Delta M_{B_s}^{\text{G2HDM}} = \Delta M_{B_s}^{\text{SM}} \left(1 + \frac{M_{12}^{\text{NP}}}{M_{12}^{\text{SM}}} \right), \tag{3.25}$$

where $\Delta M_{B_s}^{\text{SM}} = (18.2_{-0.8}^{+0.6})\,\text{ps}^{-1}$ is the SM prediction from ref. [90] and

$$M_{12}^{\text{NP}} = \frac{\left\langle B_s \left| \mathcal{H}_{\text{eff}}^{\text{NP}} \right| \overline{B}_s \right\rangle}{2\,M_{B_s}}, \tag{3.26}$$
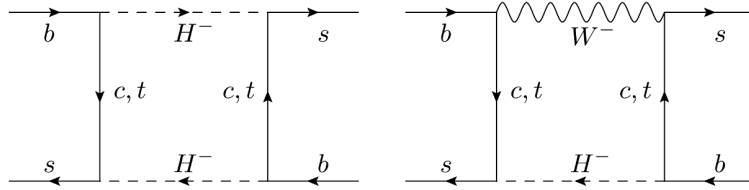
Figure 1. Box diagrams relevant for $B_s - \overline{B_s}$ mixing.

.

$$M_{12}^{\text{SM}} = \frac{G_F^2\, m_W^2 M_{B_s} f_{B_s}^2 \mathcal{B}_{B_s} \eta_B}{12\pi^2} \left(V_{tb} V_{ts}^*\right)^2 S_0, \tag{3.27}$$

are the off-diagonal 12 terms (often called dispersive terms) of the evolution matrix responsible for $B_s - \bar{B}_s$ mixing obtained from the expected value of the respective effective Hamiltonian $\mathcal{H}_{\text{eff}}^{\text{NP}}$ in eq. (4.9) of ref. [26]. M_{B_s} is the mass of the B_s meson, the parameter $\mathcal{B}_{B_s} \approx 0.841$ is the so-called *bag factor*, $\eta_B = 0.8393 \pm 0.0034$ is due to QCD corrections and $S_0 \approx 2.35$ is an Inami-Lim function [100] including electroweak corrections.

Using both the theoretical expressions of refs. [14, 26] and doing an independent calculation with `FeynCalc` [101] with the model files provided by `FeynRules` [102] as a cross-check, we compute the G2HDM contribution to the mass difference at one loop level. For simplicity, we show here the resultant expressions evaluated at the charged Higgs mass $m_{H^\pm} = 130\,\text{GeV}$, even though later we use the full expression depending on $m_{H^\pm}$ in the scans. We find for

$$\begin{aligned}
\Delta M_{B_s}^{\text{G2HDM}}/\Delta M_{B_s}^{\text{SM}} \approx{} & -0.0055|\rho_u^{tc}|^2 + 1.73|\rho_u^{tt}|^2 - 0.9\,\rho_u^{tc*}\rho_u^{tt} \\
& + 87\rho_u^{tc}\rho_u^{cc}(|\rho_u^{cc}|^2 - |\rho_u^{tc}|^2) + 1046|\rho_u^{cc}|^2|\rho_u^{tc}|^2,
\end{aligned} \tag{3.28}$$

where the first and second lines are the quadratic and quartic terms related to the W–H^- and H^-–H^- box diagrams in figure 1, respectively.[7]

3.6 Lepton flavour (universality) violation

The lepton flavour universality violation test is defined as the ratio

$$\left(\frac{g_\mu}{g_e}\right)^2 = \frac{\text{BR}(\tau \to \mu\bar{\nu}\nu)}{\text{BR}(\tau \to e\bar{\nu}\nu)} \frac{f(m_e^2/m_\tau^2)}{f(m_\mu^2/m_\tau^2)} \approx 1 + \sum_{i,j=\mu,\tau} \left(0.25\,|R_{ij}|^2 - 0.11\,\text{Re}(R_{ij})\right), \tag{3.29}$$

where g_e and g_μ are the $W^\pm$–e and $W^\pm$–μ couplings and $f(x) = 1 - 8x + 8x^3 - x^4 - 12x^2 \log x$ and R_{ij} is the BSM scalar contribution for the test of lepton flavour universality in the tau sector. In the G2HDM at tree level[8] we have

$$R_{ij} = \frac{v^2}{2\,m_{H^\pm}^2}\, \rho_\ell^{\tau i}\, \rho_\ell^{j\mu*}. \tag{3.30}$$

---

[7]Regarding the width difference $\Delta\Gamma_s$ of the $B_s - \overline{B_s}$ system, we corroborated that the contribution of NP to the CP violating phase ϕ_s^Δ in ref. [100] is negligible given that we do not consider complex Yukawa couplings except for $\rho_\ell^{\tau\tau}$.

[8]We confirmed that the dominant contributions coming from one-loop diagrams [12, 103, 104] are negligible for $|\rho_\ell^{\tau\tau}| < 0.2$.

The corresponding experimental measurement is taken from the latest Belle II data, $|g_\mu/g_e| = 0.9974 \pm 0.0019$ [31].

In the G2HDM lepton flavour violating decays of τ and μ leptons are induced by one-loop diagrams and enhanced 2-loop diagrams known as Barr-Zee contributions [105–107]. Here we use the expressions from ref. [18] for the predictions of $\tau \to \mu\gamma$, $\tau \to 3\mu$ and $\mu \to e\gamma$. They are compared to the upper experimental limits from the PDG [1] and the MEG II collaboration [108].

For the Higgs LFV decays we follow ref. [24] and use

$$\mathrm{BR}(h \to l\tau) = \frac{c_{\beta\alpha}^2 m_h}{16\pi\,\Gamma_h} \left(|\rho_\ell^{l\tau}|^2 + |\rho_\ell^{\tau l}|^2 \right), \tag{3.31}$$

where $l = e$, μ, with experimental bounds provided by CMS and ATLAS [109, 110]. Note this data also contains anomalies, but here we do not consider these and instead simply apply them as the upper limits presented in refs. [109, 110].

3.7 Higgs searches at colliders

The relative coupling strength κ_τ for $h\tau\bar{\tau}$ is defined as the ratio $\kappa_\tau^2 \equiv \Gamma_\tau/\Gamma_\tau^{\mathrm{SM}}$ where Γ_τ is the partial decay width into a pair of taus, and measured to be $\kappa_\tau = (0.93 \pm 0.07)$ by ATLAS [111] and $\kappa_\tau = (0.92 \pm 0.08)$ by CMS [112]. It is affected in the G2HDM as

$$\kappa_\tau = \left| s_{\beta\alpha} + \frac{\rho_\ell^{\tau\tau} c_{\beta\alpha}}{\frac{\sqrt{2}m_\tau}{v}} \right|. \tag{3.32}$$

Concerning direct search for the new Higgs bosons, H, A and $H^\pm$, we use the exclusion limits computed by HiggsBounds [113–116] and HiggsSignals [117, 118]. In addition, we add the limits from searches for heavy Higgses with flavour-violating couplings, not presently included in HiggsBounds or HiggsSignals. Here, the ATLAS search for the production of a heavy Higgs decaying via flavour-violating couplings resulting in a pair of same-sign tops can set a strong lower limit on the masses of heavy Higgses [119]. Nevertheless, this limit is not very effective in our study since we have no mixing between the first and third generation, $\rho_u^{tu} = 0$, and the off-diagonal Yukawas are small, $\rho_u^{tc} < 0.5$. The CMS search for the production of two heavy Higgses from off-shell Z, decaying to four taus excludes the possibility of fitting the anomalous magnetic moment of the muon (see below) in the lepton-specific 2HDM [120].[9] The limits provided on the cross sections and branching ratios can be re-interpreted in a model-agnostic way, and thus applied to our scenario. However, departing from the limit of the lepton-specific 2HDM, the di-Higgs production from an off-shell Z is generically small, such that the effect of the constraint is weakened. Moreover, in our scenario, due to the presence of additional quark Yukawa couplings, the tauonic branching ratio is diluted.

3.8 Oblique parameters and m_W mass

The oblique parameters S, T and U [123, 124] parameterise NP correction to the electroweak gauge boson propagators. In particular, they are sensitive to the W mass if the EW sector

---

[9]Moreover, the reinterpretation of neutralino search resulting in multi-taus and missing energy by AT-LAS [121] excludes the scenario too [122].

of the SM is fixed via G_F, α and the Z mass. However, the situation for the W mass measurement is not clear at the moment. While the CDF-II collaboration found a m_W value [125] which is 7σ above the SM prediction, the measurements from LEP [126], D0 [127] and the LHC [128, 129] included in the PDG average [1] are in better agreement with the SM. Furthermore, very recently the CMS collaboration reported a preliminary result of m_W consistent with the EW global fit of the SM [130], with a precision comparable with the one from CDF-II.

There are significant tensions between the LHC and the CDF-II measurements, resulting in a poor compatibility when all the measurements are combined [131]. Out of all possible combinations where a single measurement is removed, the best compatibility is obtained without the CDF-II measurement [131]. Therefore, we consider as the default option that in which CDF-II is disregarded, leading to

$$\text{PDG}: \; S = -0.04 \pm 0.10, \;\; T = 0.01 \pm 0.12, \;\; U = -0.01 \pm 0.09, \tag{3.33}$$

with correlation matrix ρ given by,

$$\rho^{\text{PDG}} = \begin{pmatrix} 1 & 0.93 & -0.70 \\ 0.93 & 1 & -0.87 \\ -0.70 & -0.87 & 1 \end{pmatrix}. \tag{3.34}$$

However, we also compare our results to the alternative case in which only the CDF-II measurement is used, resulting in [132]

$$\text{CDF}: \; S = 0.06 \pm 0.10, \;\; T = 0.11 \pm 0.12, \;\; U = 0.14 \pm 0.09, \tag{3.35}$$

with correlations

$$\rho^{\text{CDF}} = \begin{pmatrix} 1 & 0.90 & -0.59 \\ 0.90 & 1 & -0.85 \\ -0.59 & -0.85 & 1 \end{pmatrix}. \tag{3.36}$$

Here we use the 2HDMC 1.8 package [133] to include these constraints where general expressions for the S, T and U parameters from refs. [134, 135] are used. Unless otherwise explicitly stated, we use the PDG values for the S, T and U parameters from eq. (3.33).

3.9 Anomalous magnetic moment of the muon: $(g-2)_\mu$

While the situation for the direct experimental measurement of $(g-2)_\mu$ is clear [136, 137]

$$a_\mu^{\text{Exp}} = (11659205.9 \pm 2.2) \times 10^{-10}, \tag{3.37}$$

the SM prediction is puzzling. The SM value of $a_\mu^{\text{WP}} = (11659181.0 \pm 4.3) \times 10^{-10}$ computed by the $g-2$ Theory Initiative's White Paper (WP) [138], which is based on work from [139–158], gives a deviation,

$$\Delta a_\mu^{\text{WP}} = (24.9 \pm 4.8) \times 10^{-10}, \tag{3.38}$$

which is a 5.1σ tension with the direct measurement. However, that prediction does not include the BMW lattice calculation for the Hadronic Vacuum Polarisation (HVP) contribution [159, 160]. Replacing the HVP contribution from the WP with the latest BMW calculation results in

$$\Delta a_\mu^{\mathrm{BMW}} = (4.0 \pm 4.4) \times 10^{-10}. \tag{3.39}$$

The BMW calculation has been confirmed by other lattice groups [161–164] in an intermediate Euclidean time window [165]. Note also that the recent CMD-3 [166] measurement of $e^+e^- \to$ hadrons, gives systematically larger cross-section than BaBar [167] and KLOE [168]. Finally, τ-data driven results are also consistent with the lattice calculations [169, 170]. Therefore, we will use the BMW value for the fit in the main text but show the impact if a large NP effect from the G2HDM in $(g-2)_\mu$ was preferred in the appendices, namely we show in appendix A the different contributions from the model and in appendix B the results obtained if using the WP value.

4 Results

We now perform a global fit of the G2HDM to the observables discussed in section 3, using the GAMBIT [32, 33] framework. For this, we extend the FlavBit [171], PrecisionBit [172] and ColliderBit [173] modules of GAMBIT to compute the observables and likelihoods for the G2HDM as described in the previous section. We also make use of various external codes: SuperIso 4.1 [52–54, 174] for computing flavour observables, 2HDMC 1.8 [133] for precision electroweak constraints, HEPLike [92] for likelihoods of $b \to s\ell^+\ell^-$ observables. We employ the differential evolution sampler Diver 1.0.4 [175] to explore the parameter space[10] and the plotting script pippi [176] to produce all the figures below. To validate the implementation of the observables, we confirmed that the predictions for them calculated by GAMBIT (see table 1) agree with ref. [24] within the corresponding theoretical and parametric errors for one of the benchmark scenarios presented there (henceforth called "BM3"). Some small differences are due to different choices of the SM predictions vs experimental input.

To provide more information on the impact of different observables and parameters we perform multiple fits. First, we consider only the parameters used in ref. [24] with a limited set of observables to examine how the charged-current B anomalies can be explained and to study the implications for $b \to s\ell^+\ell^-$ data. We then perform a more comprehensive fit, including additional observables and increasing the number of Yukawa parameters. In our main analysis we treat $(g-2)_\mu$ and the W mass as *constraints* on new physics, using the BMW prediction for HVP contributions [160] for the former, and the oblique parameters [1] from fits that exclude the CDF-II measurement for the latter. However, we also compare this to another fit showing the impact of using the CDF-II measurement instead. Similarly, for the purpose of comparison, in the appendices, we show how results change if we instead use the HVP contributions given in the White Paper, which implies a preference for a significant BSM contribution.

In our first scan we consider the reduced parameter space of $\{m_{12}, m_{H^\pm}, m_A, m_H, s_{\beta\alpha}, \tan\beta, Y_u^{2,tt}, Y_u^{2,tc}, Y_\ell^{2,\tau\tau}, Y_\ell^{2,\mu\tau}, Y_\ell^{2,e\tau}\}$ which matches the parameters considered in ref. [24].

---

[10]The results of all the scans, ran in the LUMI supercluster in Kajaani, Finland, accumulated a total of 60 million parameter samples from 10 independent scans, using approximately 2400 CPU hours.
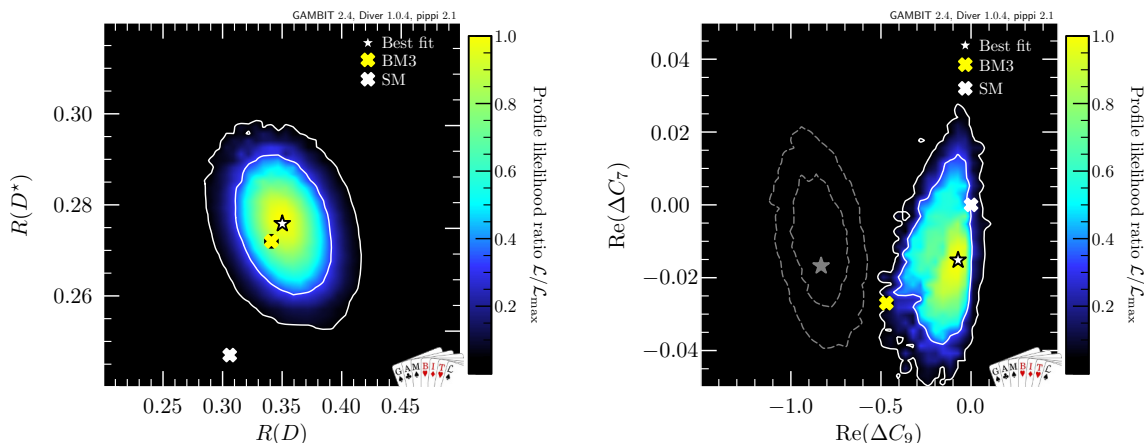
Figure 2. Profile likelihood ratios for $R(D)$ and $R(D^*)$ (left) and ΔC_9 and ΔC_7 (right). The white star with a black border denotes the best-fit point, the white cross the SM prediction, and the yellow cross corresponds to BM3 from ref. [24]. White contours around the best-fit point are the 1σ and 2σ confidence intervals (calculated with two degrees of freedom). The grey contours on the right shows the region preferred by the model-independent fit to $b \to s\ell^+\ell^-$ transitions.

For this, we exclude $b \to s\ell^+\ell^-$ from the fit and predict the contribution to the WCs of the relevant effective operators i.e. $\Delta C_{9,7}$. The resulting profile likelihood ratio is shown in figure 2, where the best-fit point is marked with a white star and the white contours are the boundaries of the 1σ and 2σ regions. Also the benchmark point 3 (BM3) of ref. [24] is depicted in yellow and the SM prediction in white. The panel on the left shows that a good fit to $R(D^*)$ can be obtained. The panel on the right illustrates that despite disregarding $b \to s\ell^+\ell^-$ data, the fit has a preference for negative values of ΔC_9, in agreement with the model-independent fit (grey contours) [5, 177]. However, the magnitude of ΔC_9 is significantly smaller within this setup compared to the one obtained from the model-independent fit. Hence, we will consider if extending the set of parameters can resolve this tension.

Therefore, we now perform a more comprehensive global fit including the additional free parameters $Y_u^{2,cc}$, $Y_d^{2,bb}$ and $Y_\ell^{2,\mu\mu}$, with the ranges described in eq. (2.18). Note that the $Y_f^{2,ba}$ couplings are only used in an intermediate step as they are the pre-implemented scan parameters in GAMBIT. For facilitating comparison with ref. [24] we show all our results in the Higgs basis, i.e. in terms of the ρ_f^{ba} couplings instead, which are derived from the $Y_f^{2,ba}$ via eq. (2.13). In this scan we also include $b \to s\ell^+\ell^-$ data, $R_{e/\mu}$, the meson decays $\mathrm{BR}(D_s \to \mu\bar{\nu})$ and $\mathrm{BR}(D_s \to \tau\bar{\nu})$, the universality test g_μ/g_e, and the new ATLAS upper limit on $t \to \mu^+\tau^-c$. For $(g-2)_\mu$ we use the SM prediction with the value of the HVP contribution obtained by BMW [160]. Note that this observable serves as a constraint since it agrees at the 0.9σ level with the measurement. The results of this fit are shown in figure 3. The best-fit point and some predictions of selected observables can be seen in the third column of table 1.

From the top-right panel of figure 3 it can be seen that it is possible to obtain $\Delta C_9 \approx -0.9$, i.e. the best-fit point of the model-independent fit, while simultaneously explaining $R(D^{(*)})$ at the 1σ level (top-left) with the extended parameter set. This means that the additional Yukawa couplings, not considered in ref. [24], are in fact capable of resolving the tension between $b \to s\ell^+\ell^-$ data and the rest of the observables within the global fit. The middle-left
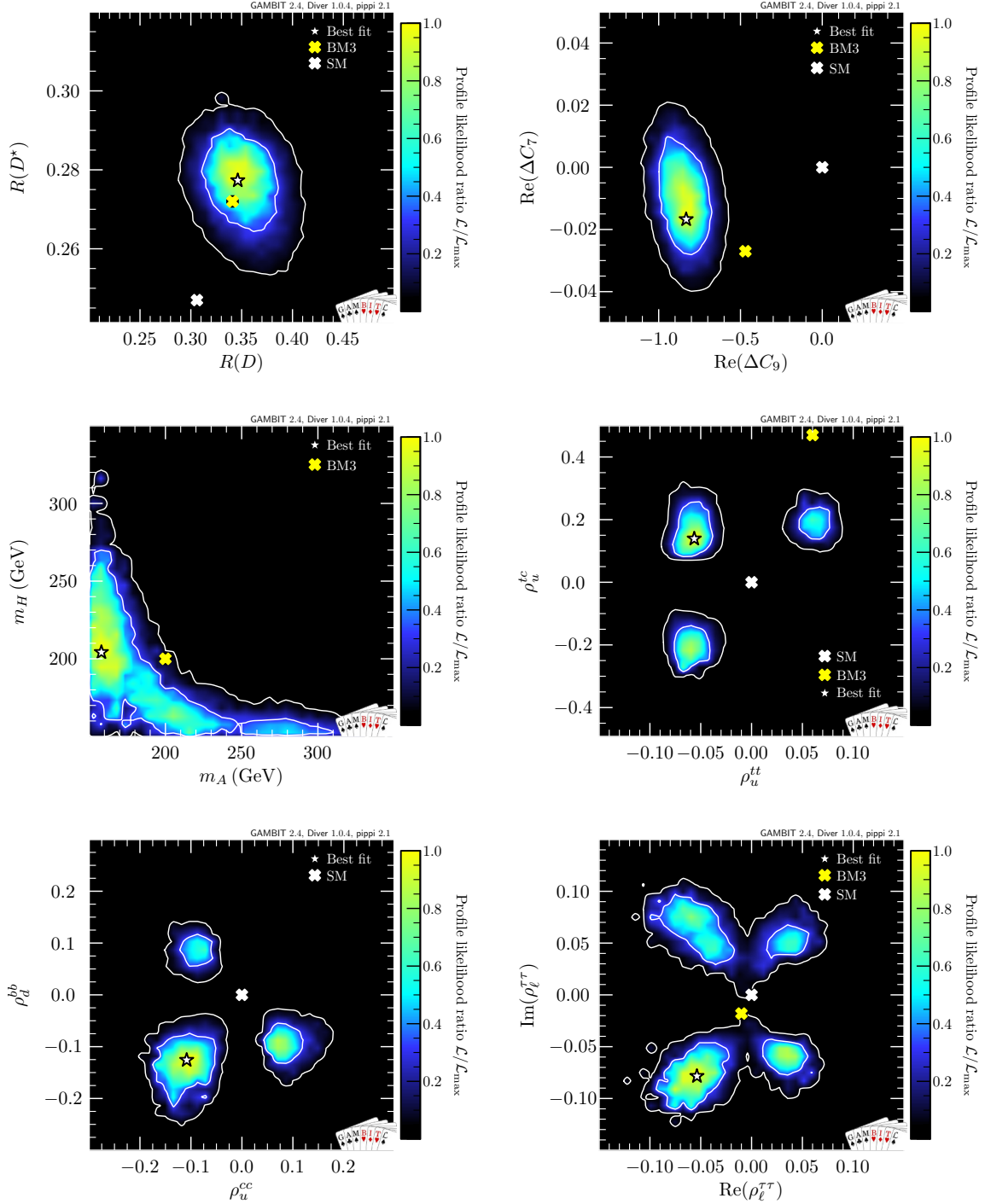
Figure 3. Profile likelihood ratio for different combinations of model parameters and observables for the full fit with the extended parameter set. As before the white star with a black border denotes the best-fit point, the white cross the SM prediction, and the yellow cross corresponds to BM3 from ref. [24]. White contours around the best fit point are the 1σ and 2σ confidence intervals.
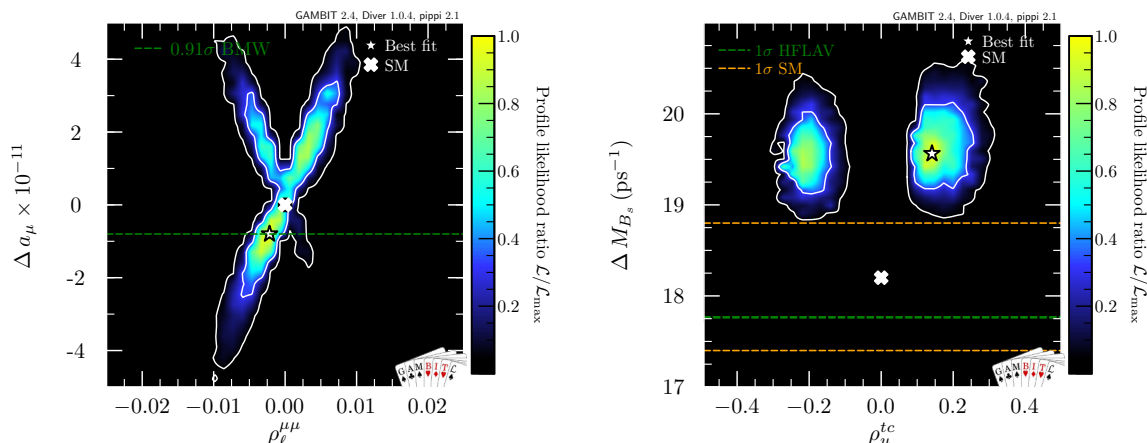
Figure 4. Profile likelihood ratios for Δa_μ (left) and ΔM_{B_s} (right) obtained from the full scan. As before the white star with a black border denotes the best-fit point and the white cross the SM prediction. White contours around the best fit point are the 1σ and 2σ confidence intervals.

panel shows the preferred region in the m_A–m_H plane which is sensitive to the S, T and U parameters. We can see a mild preference for a light m_A and slightly heavier m_H at around $200\,\mathrm{GeV}$, though degenerated masses or inverted hierarchies are also possible within 2σ of the best-fit point.[11]

Regarding the additional neutral scalars, ATLAS recently searched for a new particle decaying to $b\bar{b}$ in top decays [178]. They set an upper limit on $\mathrm{BR}(t \to cb\bar{b}) \leq \mathcal{O}(10^{-3})$ depending on the resonant mass. For the best-fit point we obtain $\mathrm{BR}(t \to cA \to cb\bar{b}) \approx 10^{-4}$, satisfying the constraint. However, for a lighter A and larger ρ_u^{tc}, this exotic top decay channel already probes the model. Note that the correction to the oblique parameters involves all additional Higgs masses and when we set $m_{H^\pm}$ close to $130\,\mathrm{GeV}$, this makes the values of m_H and m_A different compared to the case of not having the ATLAS excess.

The disjoint preferred regions in the ρ_u^{tc}–ρ_u^{tt}, ρ_d^{bb}–ρ_u^{cc} and $\mathrm{Im}\,(\rho_\ell^{\tau\tau})$–$\mathrm{Re}\,(\rho_\ell^{\tau\tau})$ planes (middle right and bottom panels) can be understood as the overlap of the functions associated to ΔC_7, ΔC_9 and $R(D^{(*)})$ defined in eqs. (3.23), (3.24), eq. (3.18) and eq. (3.11), respectively. Even though the sign of ρ_u^{tt} and ρ_d^{bb} are not fixed by the exotic top decay, the relative sign can be fixed with flavour observables. As a result, we get two independent regions (with opposite sign of ρ_u^{tc}) which is observed on the middle-right panel. Lastly, the bottom-right panel shows that a small but non-zero value of the imaginary part of $\rho_\ell^{\tau\tau}$ is necessary to explain $R(D^*)$ while simultaneously satisfying Higgs coupling strength constraints.

On the left panel of figure 4, our fit finds a small $\rho_\ell^{\mu\mu}$ and a tiny ($\mathcal{O}(10^{-11})$) shift in the muon $g-2$. On the other hand, the right-hand panel shows that the G2HDM provides a worse fit to ΔM_{B_s} than the SM, but which is still compatible with it at the 2σ level due to the large theoretical uncertainty of the SM (dashed orange lines). In the plot, the HFLAV experimental average is shown which, compared to the theory prediction, has negligible uncertainties not distinguishable on the plot as they are given by $\Delta M_{B_s}^{\mathrm{HFLAV}} = (17.765 \pm 0.006)\,\mathrm{ps}^{-1}$. The

---

[11]We, however, checked that the fit to all flavour and S, T and U parameters is almost unaffected by the exchange of m_H and m_A which suggests there may be an undersampling of the parameter space around $m_A = 250\,\mathrm{GeV}$. Nevertheless we expect that this does not change our main result i.e. $\Delta C_9 \approx -0.9$ is allowed in the model.
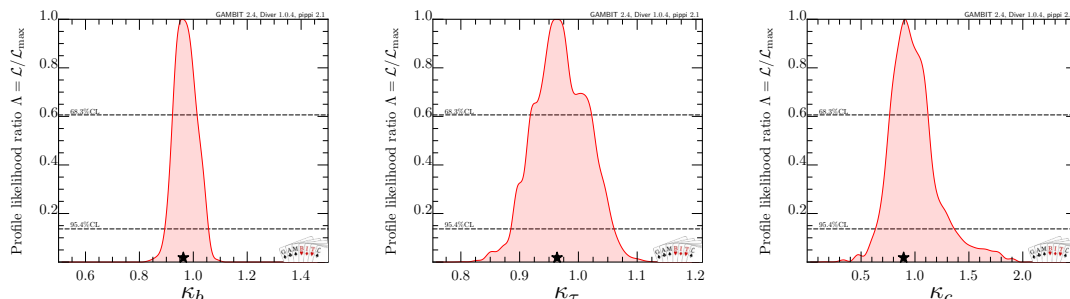
Figure 5. One-dimensional profile likelihood ratios $\mathcal{L}/\mathcal{L}_{\max}$ for the Higgs coupling strength of the bottom quarks, tau lepton, and charm quarks from left to right.
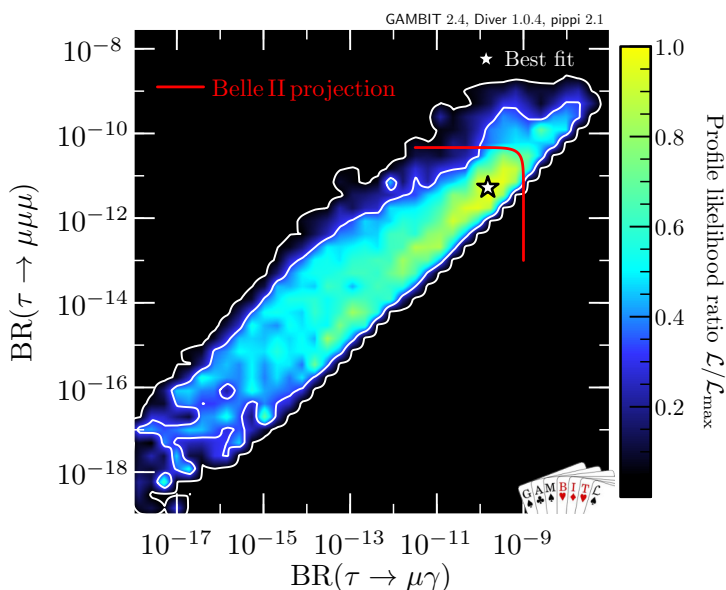

Figure 6. Profile likelihood ratios for LFV decays and projected limit from Belle-II (red solid curve). The white star denotes the best-fit point and the white contours around it are the 1σ and 2σ confidence intervals.

fit could be improved by the inclusion of small ρ_d^{bs} and ρ_d^{sb} couplings which give rise to tree-level effects in $B_s - \bar{B}_s$ mixing.

The predictions for the SM Higgs coupling strengths for tau leptons and charm and bottom quarks, $\kappa_{\tau,b,c}$ are shown in figure 5. We see that the deviation from unity in κ_τ and κ_b can be about 10%, and as high as 30% for κ_c. Note that the current uncertainty of κ_τ and κ_b is about 10% but the high luminosity (HL)-LHC will shrink those uncertainties to 4% and 2%, respectively [179]. On the other hand, we would need future lepton colliders to probe κ_c at less than 10% [179, 180] in order to test our prediction.

Figure 6 shows the predictions for the LFV decays $\tau \to \mu\gamma$ and $\tau \to 3\mu$ in the G2HDM. Both of the branching ratios are within 2σ of the future sensitivity limit from Belle II [181].[12]

---

[12]However, this is not the best possible scenario, and an even more promising projection could be obtained when using the LFV measurement obtained by the ATLAS collaboration [110] deviating 2.5σ from the SM rather than the upper limits, which we use here as a conservative approach.

Concerning LFV B decays, we find that the branching ratios of $B^{(+)} \to K^{*(+)}\mu\tau$ and $B_s \to \mu\tau$ (and also for the flavour conserving $B^{(+)} \to K^{*(+)}\tau^+\tau^-$ and $B_s \to \tau^+\tau^-$) are two orders of magnitude below the future sensitivity projection from both Belle II and the HL-LHC and do not display them here. We also note that the resulting $B_s \to \mu^+\mu^-$ branching ratio turns out to be the SM-like. Lastly, regarding the branching ratio of the $D_s \to \tau\bar{\nu}$ decay we find $\mathrm{BR}(D_s \to \tau\bar{\nu}) = 5.22 \times 10^{-2}$ for the best fit point value, which is within the experimental uncertainty at 1σ level.

Finally, we assess the impact of using the W mass from CDF-II as input in the global fit instead of the PDG value. For this, we compare the third and fourth columns in table 1 the best-fit values using the m_W from the PDG to the one using CDF-II result. We see that the NP effect in both the neutral and charged current B anomalies becomes more constrained when using the CDF-II measurement compared to the PDG value. We also show in the last row of table 1 the values for the Wilks theorem ratio test $\Delta\chi^2 = \chi^2_{\mathrm{SM}} - \chi^2_{\mathrm{G2HDM}}$,[13] showing that a much better fit to the data is obtained for the scan using the PDG values. Notably, the CDF-II fit predicts a much smaller branching ratio for the $B_c \to \tau\bar{\nu}$ decay compared to others due to $|\mathrm{Im}\left(C_L^{cb}\right)| \gg |\mathrm{Re}\left(C_L^{cb}\right)|$ which needs Tera-Z factories to probe the scenario [183–185].

5   Conclusions

Explaining the anomalies in semi-leptonic B decays remains a challenge for model building. In fact, after the disappearance of deviations from unity in the ratios $R(K^{(*)})$ testing lepton flavour phenomenology, this has become even more difficult and fewer NP models remain valid [3]. One of them is the 2HDM with a generic flavour structure. We show that it is possible to describe both the charged and neutral current anomalies in semi-leptonic B decays at the 1σ level within the G2HDM, while satisfying the experimental constraints. We do this by performing a global fit via GAMBIT that includes the constraints from all other flavour observables, top decays and electroweak precision observables. For the latter, we used the W mass from the PDG (which does not include the CDF-II measurement) and the SM prediction for $(g-2)_\mu$ with the HVP contribution calculated by the BMW collaboration, which both imply good agreement between SM and experiment so that these observables act as constraints on new physics.

We stress that the value used for the HVP contributions to $(g-2)_\mu$ plays a crucial role here. Specifically, using the BMW calculation, which implies a SM prediction close to the measured $(g-2)_\mu$ value, allows a simultaneous explanation of $R(D^{(*)})$ and $b \to s\ell^+\ell^-$ data. If instead the SM $(g-2)_\mu$ value of the White Paper is used without updating the HVP contributions, the combined fit can no longer describe both B anomalies while generating a larger Δa_μ of about 1×10^{-9} (which is still significantly smaller than the White Paper prediction). Similarly, if the PDG value for the W mass is replaced by the CDF-II measurement, the model could not fit the oblique parameters while at the same time improving the fit to the semi-leptonic B anomalies as much as before.

---

[13]For nested hypothesis $H_0 \subset H_1$ Wilks theorem [182] states that $\Delta\chi^2$ will follow a χ^2 distribution with n degrees of freedom, where n is the difference in dimensionality between the larger parameter space (G2HDM) and the nested one (SM).

	BM3	Scan 1	PDG 2024	CDF-II
m_{H^+}	130 GeV	133.7 GeV	126.2 GeV	133 GeV
$m_{H,A}$	200 GeV	181.7, 184.2 GeV	205, 158 GeV	227, 201 GeV
$c_{\beta\alpha}$	0.1	0.019	0.007	0.03
ρ_u^{tt}	0.06	0.06	-0.06	-0.06
ρ_u^{tc}	0.47	0.23	0.14	-0.15
ρ_u^{cc}	-	-	-0.1	0.1
ρ_d^{bb}	-	-	-0.07	0.1
$\rho_\ell^{\tau\tau}$	$-0.01(1 \pm 1.8\,i)$	$-0.03(1 \pm 1.5\,i)$	$-0.05(1 \pm 1.6\,i)$	$-0.002(1 \pm 25\,i)$
$\rho_\ell^{\mu\mu}$	-	-	-0.0015	0.002
$\rho_\ell^{\mu\tau}$	0.01	5×10^{-4}	0.003	-0.001
$\rho_\ell^{e\tau}$	0.006	0.008	3×10^{-4}	0.007
$\text{BR}(t \to b\bar{b}c)$	0.163%	0.157%	0.156%	0.157%
$\text{BR}(h \to \mu\tau)$	0.077%	6.7×10^{-8}	3.5×10^{-7}	6.8×10^{-7}
$\text{BR}(h \to e\tau)$	0.028%,	2.1×10^{-5}	3.6×10^{-9}	2.8×10^{-5}
$R(D)$	0.357	0.350	0.346	0.371
$R(D^*)$	0.271	0.276	0.277	0.258
$\text{BR}(\mu \to e\gamma)$	2.2×10^{-13}	1.7×10^{-15}	7.6×10^{-17}	3.1×10^{-15}
R_{B_s}	0.002	-0.005	0.075	0.062
$\text{BR}(B_c \to \tau\bar{\nu})$	30%	39%	40%	8%
$\text{BR}(t \to ch)$	3.1×10^{-4}	2.4×10^{-6}	1.4×10^{-7}	2.2×10^{-6}
ΔC_9	-0.47	-0.072	-0.83	-0.76
ΔC_7	-0.035	-0.015	-0.016	-0.011
κ_τ	0.91	0.95	0.97	1.00
Δa_μ^{BMW}	-	-	-0.8×10^{-11}	1.2×10^{-11}
$STU\ (\Delta\chi^2)$	-2.5	0.014	-0.06	-11.5
Total $\Delta\chi^2$	2.20	23.83	81.07	64.30

Table 1. The value of the parameters for BM3 (first column), the best-fit point of the first scan (second column), the best-fit point of the second scan with using the PDG value (third column) or the CDF-II value (fourth column) for the value of m_W. The corresponding predictions for various observables are shown, where relevant. Here we define $\Delta\chi^2 = \chi^2_{\text{SM}} - \chi^2_{\text{G2HDM}}$.

Interestingly, we found that if we do not include $b \to s\ell^+\ell^-$ in the fit but predict it from the other observables within the G2HDM, a negative value of ΔC_9, as suggested by global model-independent fits, is predicted, even though the absolute value is smaller than what is preferred by data. In all scenarios describing the B anomalies at the 1σ level, we find that ΔM_{B_s} is in worse agreement with data than the SM, even though still compatible due to the large theoretical uncertainty. Finally, our model can be tested at Belle II in LFV searches for $\tau \to 3\mu$ and $\tau \to \mu\gamma$ and measurements of κ_b and κ_τ in the future HL-LHC.
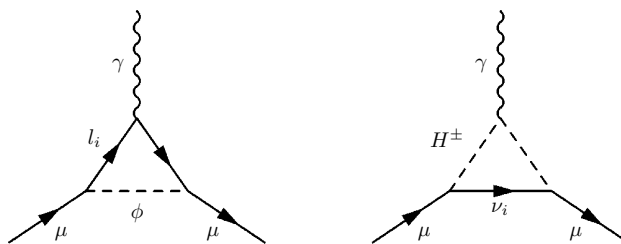
Acknowledgments

Figure 7. One-loop diagrams that contribute to $(g-2)_\mu$ involving a neutral (charged) scalar diagram on the left (right). The index $i = e, \mu, \tau$ and $\phi = h, H, A$ are defined.

A Barr-Zee diagrams for $(g-2)_\mu$ in the G2HDM

We divide the leading contributions to Δa_μ in the G2HDM into three groups

$$\Delta a_\mu^{\text{BSM}} = \Delta a_\mu^{1\text{L}} + \Delta a_\mu^F + \Delta a_\mu^B, \tag{A.1}$$

which correspond to the one-loop, two-loop fermionic, and two-loop bosonic contributions, respectively. These are shown in figures 7–10 and the corresponding expressions for the G2HDM are given in refs. [18, 186].

The two-loop fermionic Barr-Zee diagrams are shown in figure 8 and can be divided into neutral and charged contributions

$$\Delta a_\mu^F = \Delta a_\mu^{F,\text{neutral}} + \Delta a_\mu^{F,\text{charged}}. \tag{A.2}$$

The two-loop bosonic contributions can be split up further into three groups

$$\Delta a_\mu^B = \Delta a_\mu^{\text{B, EW add}} + \Delta a_\mu^{\text{B, Yuk}} + \Delta a_\mu^{\text{B, non-Yuk}}. \tag{A.3}$$

The first term $\Delta a_\mu^{\text{B,EW add}}$ represents BSM contributions from two-loop bosonic diagrams where only SM particles and the SM-like Higgs boson h appear in the loops, i.e. the left panel of figure 9 with $\phi = h$ and $H^\pm$ replaced with $W^\pm$ and the diagrams in figure 10 with $\phi = h$. BSM effects enter here because in the G2HDM h can have non-SM effects. However to avoid double counting and get only the BSM contribution we must subtract from this the SM value of these diagrams. The second term $\Delta a_\mu^{\text{B, Yuk}}$ includes all diagrams that involve BSM fields with a Yukawa coupling, e.g. the $\phi \neq h$ versions of both the diagram in the left panel of figure 9 and the diagrams in figure 10. The last term $\Delta a_\mu^{\text{B, non-Yuk}}$ represents two-loop
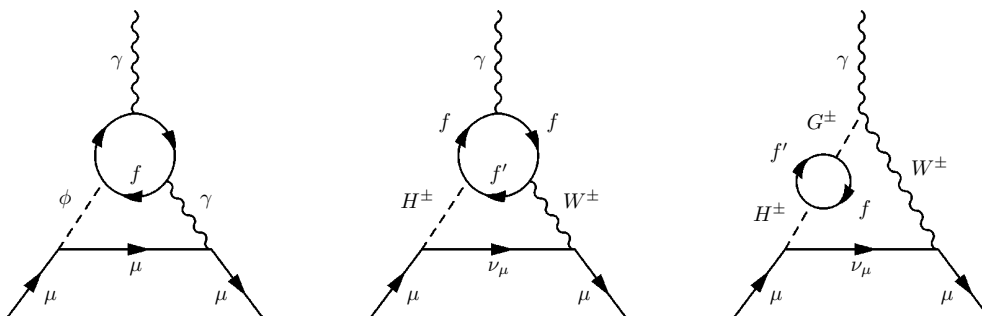
Figure 8. Two-loop fermionic Barr-Zee diagrams that contribute to $(g-2)_\mu$. The internal photon γ may be replaced by a Z boson, f' is the $SU(2)_L$ partner of f and $\phi = h, H, A$.
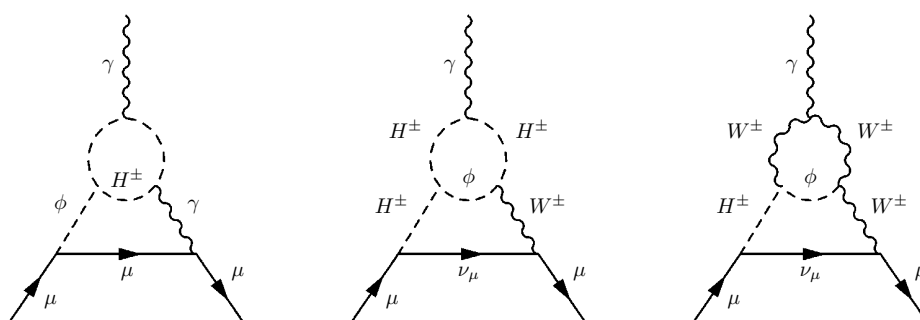

Figure 9. Two-loop bosonic Barr-Zee diagrams contributing to $(g-2)_\mu$. Here $\phi = h, H, A$, as in figure 7. In the left panel, the internal photon γ may be replaced by a Z boson, and the internal $H^\pm$ with a $W^\pm$ boson.
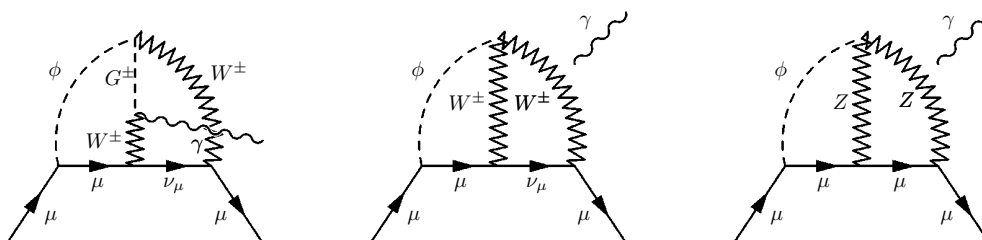

Figure 10. Two-loop bosonic 3 boson diagrams contributing to muon $g-2$. Here $\phi = h, H, A$ as in figure 7. In the middle and right panels, the detached photon could be attached to either of the vector boson lines in the diagram. In the right panel, the scalar boson ϕ may swap positions with the Z bosons.

bosonic diagrams that do not involve Yukawa couplings, such as those in the middle and right panels in figure 9. The definitions of the contributions $\Delta a_\mu^{\text{B, EW add}}$ and $\Delta a_\mu^{\text{B, non-Yuk}}$ are shown in eqs. (49) and (71) respectively in ref. [187], while the Yukawa contribution $\Delta a_\mu^{\text{B, Yuk}}$ is shown in eq. (67) of ref. [186].
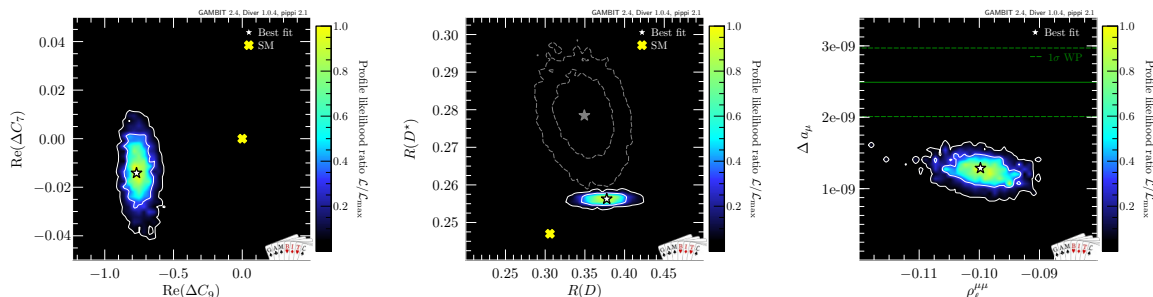
Figure 11. Profile likelihood ratios $\mathcal{L}/\mathcal{L}_{\max}$ for different 2D plots of the parameter space for the scan using the WP value for muon $g-2$. The grey contours on the middle panel are the comparison with respect to the previous scan in section 4.

B Fit with $(g-2)_\mu$ value from White Paper

Here we present the results of a scan using the WP value [138] for the SM prediction for the muon $g-2$ instead of the one where BMW is used for HVP. We find $|\rho_\ell^{\tau\tau}| \ll |\rho_u^{cc}|$ resulting in $\mathrm{BR}(\phi \to \tau\bar{\tau}) \ll \mathrm{BR}(\phi \to c\bar{c})$ and hence multi lepton search and chargino-neutralino searches would be less relevant. In figure 11 we can see that it is possible to simultaneously fit all observables only at the 2σ level, with the exception of $R(D^*)$ which is SM-like within this global fit. This is expected due to the smaller experimental uncertainty for the WP value (compared to the BMW one), strongly constraining the ρ_u^{tc} Yukawa coupling, although requiring a large $\rho_u^{cc} \approx -0.5$, in possible conflict with $pp \to c\bar{c} \to \phi$ and $pp \to cs \to H^\pm$ searches. Finally, we find that if using the CDF-II value for m_W the model is ruled out at the 2σ level for an explanation of the WP value in the G2HDM.

Data Availability Statement. This article has no associated data or the data will not be deposited.

Code Availability Statement. This article has no associated code or the code will not be deposited.

References

[1] Particle Data Group collaboration, *Review of particle physics*, *Phys. Rev. D* **110** (2024) 030001 [InSPIRE].

[2] A. Crivellin and B. Mellado, *Anomalies in particle physics and their implications for physics beyond the standard model*, *Nature Rev. Phys.* **6** (2024) 294 [arXiv:2309.03870] [InSPIRE].

[3] B. Capdevila, A. Crivellin and J. Matias, *Review of semileptonic B anomalies*, *Eur. Phys. J. ST* **1** (2023) 20 [arXiv:2309.01311] [InSPIRE].

[4] HFLAV collaboration, *Averages of b-hadron, c-hadron, and τ-lepton properties as of 2021*, *Phys. Rev. D* **107** (2023) 052008 [arXiv:2206.07501] [InSPIRE].

[5] M. Algueró et al., *To (b)e or not to (b)e: no electrons at LHCb*, *Eur. Phys. J. C* **83** (2023) 648 [arXiv:2304.07330] [INSPIRE].

[6] ATLAS collaboration, *Search for a light charged Higgs boson in $t \to H^{\pm}b$ decays, with $H^{\pm} \to cb$, in the lepton+jets final state in proton-proton collisions at $\sqrt{s} = 13$ TeV with the ATLAS detector*, *JHEP* **09** (2023) 004 [arXiv:2302.11739] [INSPIRE].

[7] J.F. Gunion and H.E. Haber, *The CP conserving two Higgs doublet model: The approach to the decoupling limit*, *Phys. Rev. D* **67** (2003) 075019 [hep-ph/0207010] [INSPIRE].

[8] G.C. Branco et al., *Theory and phenomenology of two-Higgs-doublet models*, *Phys. Rept.* **516** (2012) 1 [arXiv:1106.0034] [INSPIRE].

[9] A. Crivellin, C. Greub and A. Kokulu, *Explaining $B \to D\tau\nu$, $B \to D^{*}\tau\nu$ and $B \to \tau\nu$ in a 2HDM of type III*, *Phys. Rev. D* **86** (2012) 054014 [arXiv:1206.2634] [INSPIRE].

[10] A. Crivellin, A. Kokulu and C. Greub, *Flavor-phenomenology of two-Higgs-doublet models with generic Yukawa structure*, *Phys. Rev. D* **87** (2013) 094031 [arXiv:1303.5877] [INSPIRE].

[11] J.M. Cline, *Scalar doublet models confront τ and b anomalies*, *Phys. Rev. D* **93** (2016) 075017 [arXiv:1512.02210] [INSPIRE].

[12] A. Crivellin, J. Heeck and P. Stoffer, *A perturbed lepton-specific two-Higgs-doublet model facing experimental hints for physics beyond the Standard Model*, *Phys. Rev. Lett.* **116** (2016) 081801 [arXiv:1507.07567] [INSPIRE].

[13] J.-P. Lee, *$B \to D^{(*)}\tau\nu_{\tau}$ in the 2HDM with an anomalous τ coupling*, *Phys. Rev. D* **96** (2017) 055005 [arXiv:1705.02465] [INSPIRE].

[14] S. Iguro and K. Tobe, *$R(D^{(*)})$ in a general two Higgs doublet model*, *Nucl. Phys. B* **925** (2017) 560 [arXiv:1708.06176] [INSPIRE].

[15] R. Martinez, C.F. Sierra and G. Valencia, *Beyond $\mathcal{R}(D^{(*)})$ with the general type-III 2HDM for $b \to c\tau\nu$*, *Phys. Rev. D* **98** (2018) 115012 [arXiv:1805.04098] [INSPIRE].

[16] S. Fraser et al., *Towards a viable scalar interpretation of $R_{D^{(*)}}$*, *Phys. Rev. D* **98** (2018) 035016 [arXiv:1805.08189] [INSPIRE].

[17] S. Iguro, Y. Omura and M. Takeuchi, *Test of the $R(D^{(*)})$ anomaly at the LHC*, *Phys. Rev. D* **99** (2019) 075013 [arXiv:1810.05843] [INSPIRE].

[18] P. Athron et al., *Likelihood analysis of the flavour anomalies and $g - 2$ in the general two Higgs doublet model*, *JHEP* **01** (2022) 037 [arXiv:2111.10464] [INSPIRE].

[19] S. Iguro, *Revival of H- interpretation of $R_{D^{(*)}}$ anomaly and closing low mass window*, *Phys. Rev. D* **105** (2022) 095011 [arXiv:2201.06565] [INSPIRE].

[20] M. Blanke, S. Iguro and H. Zhang, *Towards ruling out the charged Higgs interpretation of the $R_{D^{(*)}}$ anomaly*, *JHEP* **06** (2022) 043 [arXiv:2202.10468] [INSPIRE].

[21] K. Ezzat, G. Faisel and S. Khalil, *Investigating R_D and R_{D^*} anomalies in a left-right model with an inverse seesaw*, *Eur. Phys. J. C* **83** (2023) 731 [arXiv:2204.10922] [INSPIRE].

[22] M. Fedele et al., *Impact of $\Lambda b \to \Lambda c\tau\nu$ measurement on new physics in $b \to c\ell\nu$ transitions*, *Phys. Rev. D* **107** (2023) 055005 [arXiv:2211.14172] [INSPIRE].

[23] N. Das, A. Adhikary and R. Dutta, *Revisiting $b \to c\tau\nu$ anomalies with charged Higgs boson*, arXiv:2305.17766 [INSPIRE].

[24] A. Crivellin and S. Iguro, *Accumulating hints for flavor-violating Higgs bosons at the electroweak scale*, *Phys. Rev. D* **110** (2024) 015014 [arXiv:2311.03430] [INSPIRE].

[25] S. Iguro and Y. Omura, *Status of the semileptonic B decays and muon g-2 in general 2HDMs with right-handed neutrinos*, *JHEP* **05** (2018) 173 [arXiv:1802.01732] [INSPIRE].

[26] A. Crivellin, D. Müller and C. Wiegand, *b → sℓ⁺ℓ⁻ transitions in two-Higgs-doublet models*, *JHEP* **06** (2019) 119 [arXiv:1903.10440] [INSPIRE].

[27] G. Kumar, *Interplay of the charged Higgs boson effects in $R_{D^{(*)}}$, $b \to s\ell^+\ell^-$, and W mass*, *Phys. Rev. D* **107** (2023) 075016 [arXiv:2212.07233] [INSPIRE].

[28] S. Iguro, *Conclusive probe of the charged Higgs solution of P_5' and $R_{D^{(*)}}$ discrepancies*, *Phys. Rev. D* **107** (2023) 095004 [arXiv:2302.08935] [INSPIRE].

[29] J. Herrero-Garcia et al., *Higgs Quark Flavor Violation: Simplified Models and Status of General Two-Higgs-Doublet Model*, *JHEP* **02** (2020) 147 [arXiv:1907.05900] [INSPIRE].

[30] ATLAS collaboration, *Search for charged-lepton-flavor violating μτqt interactions in top-quark production and decay in pp collisions at $\sqrt{s} = 13$ TeV with the ATLAS detector at the LHC*, *Phys. Rev. D* **110** (2024) 012014 [arXiv:2403.06742] [INSPIRE].

[31] BELLE-II collaboration, *Tau and low multiplicity physics at Belle and Belle II*, arXiv:2405.09974 [INSPIRE].

[32] GAMBIT collaboration, *GAMBIT: The Global and Modular Beyond-the-Standard-Model Inference Tool*, *Eur. Phys. J. C* **77** (2017) 784 [*Addendum ibid.* **78** (2018) 98] [arXiv:1705.07908] [INSPIRE].

[33] A. Kvellestad, P. Scott and M. White, *GAMBIT and its Application in the Search for Physics Beyond the Standard Model*, arXiv:1912.04079 [DOI:10.1016/j.ppnp.2020.103769] [INSPIRE].

[34] S. Iguro and Y. Omura, *The direct CP violation in a general two Higgs doublet model*, *JHEP* **08** (2019) 098 [arXiv:1905.11778] [INSPIRE].

[35] S. Banik and A. Crivellin, *Explanation of the excesses in associated di-photon production at 152 GeV in 2HDM*, *JHEP* **10** (2024) 203 [arXiv:2407.06267] [INSPIRE].

[36] ATLAS collaboration, *Search for a light charged Higgs boson in $t \to H^\pm b$ decays, with $H^\pm \to cs$, in pp collisions at $\sqrt{s} = 13$ TeV with the ATLAS detector*, arXiv:2407.10096 [INSPIRE].

[37] ATLAS collaboration, *Search for flavour-changing neutral tqH interactions with $H \to \gamma\gamma$ in pp collisions at $\sqrt{s} = 13$ TeV using the ATLAS detector*, *JHEP* **12** (2023) 195 [arXiv:2309.12817] [INSPIRE].

[38] CMS collaboration, *Search for flavor-changing neutral current interactions of the top quark and Higgs boson in proton-proton collisions at $\sqrt{s} = 13$ TeV*, CMS-PAS-TOP-22-002 (2023) [INSPIRE].

[39] LHCB collaboration, *Test of lepton flavor universality using B0→D*-τ+ντ decays with hadronic τ channels*, *Phys. Rev. D* **108** (2023) 012018 [*Erratum ibid.* **109** (2024) 119902] [arXiv:2305.01463] [INSPIRE].

[40] LHCB collaboration, *Measurement of the ratios of branching fractions $\mathcal{R}(D^*)$ and $\mathcal{R}(D^0)$*, *Phys. Rev. Lett.* **131** (2023) 111802 [arXiv:2302.02886] [INSPIRE].

[41] LHCB collaboration, *Measurement of the branching fraction ratios $R(D^+)$ and $R(D^{*+})$ using muonic τ decays*, arXiv:2406.03387 [INSPIRE].

[42] BELLE collaboration, *Measurement of the branching ratio of $\bar{B} \to D^{(*)}\tau^-\bar{\nu}_\tau$ relative to $\bar{B} \to D^{(*)}\ell^-\bar{\nu}_\ell$ decays with hadronic tagging at Belle*, *Phys. Rev. D* **92** (2015) 072014 [arXiv:1507.03233] [INSPIRE].

[43] BELLE collaboration, *Measurement of the τ lepton polarization and $R(D^*)$ in the decay $\bar{B} \to D^*\tau^-\bar{\nu}_\tau$*, *Phys. Rev. Lett.* **118** (2017) 211801 [arXiv:1612.00529] [INSPIRE].

[44] BELLE collaboration, *Measurement of the τ lepton polarization and $R(D^*)$ in the decay $\bar{B} \to D^*\tau^-\bar{\nu}_\tau$ with one-prong hadronic τ decays at Belle*, *Phys. Rev. D* **97** (2018) 012004 [arXiv:1709.00129] [INSPIRE].

[45] BELLE collaboration, *Measurement of $\mathcal{R}(D)$ and $\mathcal{R}(D^*)$ with a semileptonic tagging method*, *Phys. Rev. Lett.* **124** (2020) 161803 [arXiv:1910.05864] [INSPIRE].

[46] BELLE-II collaboration, *Test of lepton flavor universality with a measurement of $R(D^*)$ using hadronic B tagging at the Belle II experiment*, *Phys. Rev. D* **110** (2024) 072020 [arXiv:2401.02840] [INSPIRE].

[47] BABAR collaboration, *Evidence for an excess of $\bar{B} \to D^{(*)}\tau^-\bar{\nu}_\tau$ decays*, *Phys. Rev. Lett.* **109** (2012) 101802 [arXiv:1205.5442] [INSPIRE].

[48] BABAR collaboration, *Measurement of an Excess of $\bar{B} \to D^{(*)}\tau^-\bar{\nu}_\tau$ Decays and Implications for Charged Higgs Bosons*, *Phys. Rev. D* **88** (2013) 072012 [arXiv:1303.0571] [INSPIRE].

[49] HFLAV collaboration. *Preliminary average of $R(D)$ and $R(D^*)$ for Moriond 2024*, https://hflav-eos.web.cern.ch/hflav-eos/semi/moriond24/html/RDsDsstar/RDRDs.html.

[50] G.M. de Divitiis, R. Petronzio and N. Tantalo, *Quenched lattice calculation of semileptonic heavy-light meson form factors*, *JHEP* **10** (2007) 062 [arXiv:0707.0587] [INSPIRE].

[51] J.F. Kamenik and F. Mescia, *$B \to D\tau\nu$ Branching Ratios: Opportunity for Lattice QCD and Hadron Colliders*, *Phys. Rev. D* **78** (2008) 014003 [arXiv:0802.3790] [INSPIRE].

[52] F. Mahmoudi, *SuperIso: A program for calculating the isospin asymmetry of $B \to K^*$ gamma in the MSSM*, *Comput. Phys. Commun.* **178** (2008) 745 [arXiv:0710.2067] [INSPIRE].

[53] F. Mahmoudi, *SuperIso v2.3: A program for calculating flavor physics observables in Supersymmetry*, *Comput. Phys. Commun.* **180** (2009) 1579 [arXiv:0808.3144] [INSPIRE].

[54] F. Mahmoudi, *SuperIso v3.0, flavor physics observables calculations: Extension to NMSSM*, *Comput. Phys. Commun.* **180** (2009) 1718 [INSPIRE].

[55] R. Alonso, E.E. Jenkins, A.V. Manohar and M. Trott, *Renormalization Group Evolution of the Standard Model Dimension Six Operators III: Gauge Coupling Dependence and Phenomenology*, *JHEP* **04** (2014) 159 [arXiv:1312.2014] [INSPIRE].

[56] E.E. Jenkins, A.V. Manohar and M. Trott, *Renormalization Group Evolution of the Standard Model Dimension Six Operators II: Yukawa Dependence*, *JHEP* **01** (2014) 035 [arXiv:1310.4838] [INSPIRE].

[57] M. González-Alonso, J. Martin Camalich and K. Mimouni, *Renormalization-group evolution of new physics contributions to (semi)leptonic meson decays*, *Phys. Lett. B* **772** (2017) 777 [arXiv:1706.00410] [INSPIRE].

[58] J. Aebischer, M. Fael, C. Greub and J. Virto, *B physics Beyond the Standard Model at One Loop: Complete Renormalization Group Evolution below the Electroweak Scale*, *JHEP* **09** (2017) 158 [arXiv:1704.06639] [INSPIRE].

[59] BELLE collaboration, *Measurement of the CKM matrix element $|V_{cb}|$ from $B^0 \to D^{*-}\ell^+\nu_\ell$ at Belle*, *Phys. Rev. D* **100** (2019) 052007 [*Erratum ibid.* **103** (2021) 079901] [arXiv:1809.03290] [INSPIRE].

[60] C. Murgui, A. Peñuelas, M. Jung and A. Pich, *Global fit to $b \to c\tau\nu$ transitions*, *JHEP* **09** (2019) 103 [arXiv:1904.09311] [INSPIRE].

[61] M. Tanaka and R. Watanabe, *New physics in the weak interaction of $\bar{B} \to D^{(*)}\tau\bar{\nu}$*, *Phys. Rev. D* **87** (2013) 034028 [arXiv:1212.1878] [INSPIRE].

[62] J. Hernandez-Sánchez, S. Moretti, R. Noriega-Papaqui and A. Rosado, *Off-diagonal terms in Yukawa textures of the Type-III 2-Higgs doublet model and light charged Higgs boson phenomenology*, *JHEP* **07** (2013) 044 [arXiv:1212.6818] [INSPIRE].

[63] M. Jung, A. Pich and P. Tuzon, *Charged-Higgs phenomenology in the Aligned two-Higgs-doublet model*, *JHEP* **11** (2010) 003 [arXiv:1006.0470] [INSPIRE].

[64] R. Alonso, B. Grinstein and J. Martin Camalich, *Lifetime of B_c^- Constrains Explanations for Anomalies in $B \to D^{(*)}\tau\nu$*, *Phys. Rev. Lett.* **118** (2017) 081802 [arXiv:1611.06676] [INSPIRE].

[65] M. Blanke et al., *Impact of polarization observables and $B_c \to \tau\nu$ on new physics explanations of the $b \to c\tau\nu$ anomaly*, *Phys. Rev. D* **99** (2019) 075006 [arXiv:1811.09603] [INSPIRE].

[66] J. Aebischer and B. Grinstein, *Standard Model prediction of the B_c lifetime*, *JHEP* **07** (2021) 130 [arXiv:2105.02988] [INSPIRE].

[67] S. Iguro, T. Kitahara and R. Watanabe, *Global fit to $b \to c\tau\nu$ anomalies 2022 mid-autumn*, arXiv:2210.10751 [INSPIRE].

[68] A.J. Buras, *Standard Model predictions for rare K and B decays without new physics infection*, *Eur. Phys. J. C* **83** (2023) 66 [arXiv:2209.03968] [INSPIRE].

[69] S. Neshatpour, T. Hurth, F. Mahmoudi and D. Martinez Santos, *Neutral Current B-Decay Anomalies*, *Springer Proc. Phys.* **292** (2023) 11 [arXiv:2210.07221] [INSPIRE].

[70] N. Gubernari, M. Reboud, D. van Dyk and J. Virto, *Improved theory predictions and global analysis of exclusive $b \to s\mu^+\mu^-$ processes*, *JHEP* **09** (2022) 133 [arXiv:2206.03797] [INSPIRE].

[71] M. Ciuchini et al., *Constraints on lepton universality violation from rare B decays*, *Phys. Rev. D* **107** (2023) 055036 [arXiv:2212.10516] [INSPIRE].

[72] Q. Wen and F. Xu, *Global fits of new physics in $b \to s$ after the RK(*) 2022 release*, *Phys. Rev. D* **108** (2023) 095038 [arXiv:2305.19038] [INSPIRE].

[73] P. Athron, R. Martinez and C. Sierra, *B meson anomalies and large $B^+ \to K^+\nu\bar{\nu}$ in non-universal $U(1)'$ models*, *JHEP* **02** (2024) 121 [arXiv:2308.13426] [INSPIRE].

[74] S. Descotes-Genon, J. Matias, M. Ramon and J. Virto, *Implications from clean observables for the binned analysis of $B \to K * \mu^+\mu^-$ at large recoil*, *JHEP* **01** (2013) 048 [arXiv:1207.2753] [INSPIRE].

[75] LHCB collaboration, *Angular analysis of the $B^0 \to K^{*0}\mu^+\mu^-$ decay using $3 fb^{-1}$ of integrated luminosity*, *JHEP* **02** (2016) 104 [arXiv:1512.04442] [INSPIRE].

[76] LHCB collaboration, *Measurement of CP-Averaged Observables in the $B^0 \to K^{*0}\mu^+\mu^-$ Decay*, *Phys. Rev. Lett.* **125** (2020) 011802 [arXiv:2003.04831] [INSPIRE].

[77] LHCB collaboration, *Angular Analysis of the $B^+ \to K^{*+}\mu^+\mu^-$ Decay*, *Phys. Rev. Lett.* **126** (2021) 161802 [arXiv:2012.13241] [INSPIRE].

[78] CMS collaboration, *Angular analysis of the $B^0 \to K^{*0}(892)\mu^+\mu^-$ decay at $\sqrt{s} = 13\ TeV$*, CMS-PAS-BPH-21-002 (2024) INSPIRE.

[79] W. Altmannshofer et al., *Symmetries and Asymmetries of $B \to K^*\mu^+\mu^-$ Decays in the Standard Model and Beyond*, *JHEP* **01** (2009) 019 [arXiv:0811.1214] [INSPIRE].

[80] J. Bhom et al., *A model-independent analysis of b→sμ⁺μ⁻ transitions with GAMBIT's FlavBit*, *Eur. Phys. J. C* **81** (2021) 1076 [arXiv:2006.03489] [INSPIRE].

[81] LHCB collaboration, *Angular analysis and differential branching fraction of the decay $B_s^0 \to \phi\mu^+\mu^-$*, *JHEP* **09** (2015) 179 [arXiv:1506.08777] [INSPIRE].

[82] LHCB collaboration, *Branching Fraction Measurements of the Rare $B_s^0 \to \phi\mu^+\mu^-$ and $B_s^0 \to f_2'(1525)\mu^+\mu^-$- Decays*, *Phys. Rev. Lett.* **127** (2021) 151801 [arXiv:2105.14007] [INSPIRE].

[83] LHCB collaboration, *Angular analysis of the rare decay $B_s^0 \to \phi\mu^+\mu^-$*, *JHEP* **11** (2021) 043 [arXiv:2107.13428] [INSPIRE].

[84] LHCB collaboration, *Differential branching fractions and isospin asymmetries of $B \to K^{(*)}\mu^+\mu^-$ decays*, *JHEP* **06** (2014) 133 [arXiv:1403.8044] [INSPIRE].

[85] LHCB collaboration, *Measurements of the S-wave fraction in $B^0 \to K^+\pi^-\mu^+\mu^-$ decays and the $B^0 \to K^*(892)^0\mu^+\mu^-$ differential branching fraction*, *JHEP* **11** (2016) 047 [*Erratum ibid.* **04** (2017) 142] [arXiv:1606.04731] [INSPIRE].

[86] HPQCD collaboration, *Standard Model predictions for $B \to K\ell^+\ell^-$, $B \to K\ell_1^-\ell_2^+$ and $B \to K\nu\bar\nu$ using form factors from $N_f = 2 + 1 + 1$ lattice QCD*, *Phys. Rev. D* **107** (2023) 014511 [*Erratum ibid.* **107** (2023) 119903] [arXiv:2207.13371] [INSPIRE].

[87] G. Isidori, Z. Polonsky and A. Tinari, *Semi-inclusive $b \to s\bar\ell\ell$ transitions at high q^2*, *Phys. Rev. D* **108** (2023) 093008 [arXiv:2305.03076] [INSPIRE].

[88] S. Jäger, M. Kirk, A. Lenz and K. Leslie, *Charming new physics in rare B-decays and mixing?*, *Phys. Rev. D* **97** (2018) 015021 [arXiv:1701.09183] [INSPIRE].

[89] C. Bobeth et al., *On new physics in $\Delta\Gamma_d$*, *JHEP* **06** (2014) 040 [arXiv:1404.2531] [INSPIRE].

[90] A. Crivellin and M. Kirk, *Diquark explanation of $b \to s\ell^+\ell^-$*, *Phys. Rev. D* **108** (2023) L111701 [arXiv:2309.07205] [INSPIRE].

[91] S. Jäger, M. Kirk, A. Lenz and K. Leslie, *Charming New B-Physics*, *JHEP* **03** (2020) 122 [*Erratum ibid.* **04** (2023) 094] [arXiv:1910.12924] [INSPIRE].

[92] J. Bhom and M. Chrzaszcz, *HEPLike: an open source framework for experimental likelihood evaluation*, *Comput. Phys. Commun.* **254** (2020) 107235 [arXiv:2003.03956] [INSPIRE].

[93] A. Czarnecki and W.J. Marciano, *Electroweak radiative corrections to $b \to s$ gamma*, *Phys. Rev. Lett.* **81** (1998) 277 [hep-ph/9804252] [INSPIRE].

[94] M. Misiak et al., *Estimate of $\mathcal{B}(\bar B \to X_s\gamma)$ at $O(\alpha_s^2)$*, *Phys. Rev. Lett.* **98** (2007) 022002 [hep-ph/0609232] [INSPIRE].

[95] M. Misiak and M. Steinhauser, *NNLO QCD corrections to the anti-B → X(s) gamma matrix elements using interpolation in m(c)*, *Nucl. Phys. B* **764** (2007) 62 [hep-ph/0609241] [INSPIRE].

[96] M. Czakon et al., *The $(Q_7, Q_{1,2})$ contribution to $\overline{B} \to X_s\gamma$ at $\mathcal{O}\left(\alpha_s^2\right)$*, *JHEP* **04** (2015) 168 [arXiv:1503.01791] [INSPIRE].

[97] M. Misiak and M. Steinhauser, *Weak radiative decays of the B meson and bounds on $M_{H^\pm}$ in the Two-Higgs-Doublet Model*, *Eur. Phys. J. C* **77** (2017) 201 [arXiv:1702.04571] [INSPIRE].

[98] M. Misiak, A. Rehman and M. Steinhauser, *Towards $\overline{B} \to X_s\gamma$ at the NNLO in QCD without interpolation in m_c*, *JHEP* **06** (2020) 175 [arXiv:2002.01548] [INSPIRE].

[99] BELLE-II collaboration, *Evidence for $B^+ \to K^+\nu\bar\nu$ decays*, *Phys. Rev. D* **109** (2024) 112006 [arXiv:2311.14647] [INSPIRE].

[100] A. Lenz et al., *Anatomy of New Physics in $B - \bar{B}$ mixing*, *Phys. Rev. D* **83** (2011) 036004 [arXiv:1008.1593] [INSPIRE].

[101] V. Shtabovenko, R. Mertig and F. Orellana, *New Developments in FeynCalc 9.0*, *Comput. Phys. Commun.* **207** (2016) 432 [arXiv:1601.01167] [INSPIRE].

[102] C. Degrande, *Automatic evaluation of UV and R2 terms for beyond the Standard Model Lagrangians: a proof-of-principle*, *Comput. Phys. Commun.* **197** (2015) 239 [arXiv:1406.3030] [INSPIRE].

[103] M. Krawczyk and D. Temes, *2HDM(II) radiative corrections in leptonic tau decays*, *Eur. Phys. J. C* **44** (2005) 435 [hep-ph/0410248] [INSPIRE].

[104] T. Abe, R. Sato and K. Yagyu, *Lepton-specific two Higgs doublet model as a solution of muon $g - 2$ anomaly*, *JHEP* **07** (2015) 064 [arXiv:1504.07059] [INSPIRE].

[105] S.M. Barr and A. Zee, *Electric Dipole Moment of the Electron and of the Neutron*, *Phys. Rev. Lett.* **65** (1990) 21 [*Erratum ibid.* **65** (1990) 2920] [INSPIRE].

[106] T. Abe, J. Hisano, T. Kitahara and K. Tobioka, *Gauge invariant Barr-Zee type contributions to fermionic EDMs in the two-Higgs doublet models*, *JHEP* **01** (2014) 106 [*Erratum ibid.* **04** (2016) 161] [arXiv:1311.4704] [INSPIRE].

[107] V. Ilisie, *New Barr-Zee contributions to $(g - 2)_\mu$ in two-Higgs-doublet models*, *JHEP* **04** (2015) 077 [arXiv:1502.04199] [INSPIRE].

[108] MEG II collaboration, *A search for $\mu^+ \to e^+\gamma$ with the first dataset of the MEG II experiment*, *Eur. Phys. J. C* **84** (2024) 216 [*Erratum ibid.* **84** (2024) 1042] [arXiv:2310.12614] [INSPIRE].

[109] CMS collaboration, *Search for lepton-flavor violating decays of the Higgs boson in the $\mu\tau$ and $e\tau$ final states in proton-proton collisions at $\sqrt{s} = 13$ TeV*, *Phys. Rev. D* **104** (2021) 032013 [arXiv:2105.03007] [INSPIRE].

[110] ATLAS collaboration, *Searches for lepton-flavour-violating decays of the Higgs boson into $e\tau$ and $\mu\tau$ in $\sqrt{s} = 13$ TeV pp collisions with the ATLAS detector*, *JHEP* **07** (2023) 166 [arXiv:2302.05225] [INSPIRE].

[111] ATLAS collaboration, *A detailed map of Higgs boson interactions by the ATLAS experiment ten years after the discovery*, *Nature* **607** (2022) 52 [*Erratum ibid.* **612** (2022) E24] [arXiv:2207.00092] [INSPIRE].

[112] CMS collaboration, *A portrait of the Higgs boson by the CMS experiment ten years after the discovery*, *Nature* **607** (2022) 60 [arXiv:2207.00043] [INSPIRE].

[113] P. Bechtle et al., *HiggsBounds: Confronting Arbitrary Higgs Sectors with Exclusion Bounds from LEP and the Tevatron*, *Comput. Phys. Commun.* **181** (2010) 138 [arXiv:0811.4169] [INSPIRE].

[114] P. Bechtle et al., *HiggsBounds 2.0.0: Confronting Neutral and Charged Higgs Sector Predictions with Exclusion Bounds from LEP and the Tevatron*, *Comput. Phys. Commun.* **182** (2011) 2605 [arXiv:1102.1898] [INSPIRE].

[115] P. Bechtle et al., HiggsBounds $- 4$: *Improved Tests of Extended Higgs Sectors against Exclusion Bounds from LEP, the Tevatron and the LHC*, *Eur. Phys. J. C* **74** (2014) 2693 [arXiv:1311.0055] [INSPIRE].

[116] P. Bechtle et al., *Applying Exclusion Likelihoods from LHC Searches to Extended Higgs Sectors*, *Eur. Phys. J. C* **75** (2015) 421 [arXiv:1507.06706] [INSPIRE].

[117] P. Bechtle et al., *HiggsSignals: Confronting arbitrary Higgs sectors with measurements at the Tevatron and the LHC*, *Eur. Phys. J. C* **74** (2014) 2711 [arXiv:1305.1933] [INSPIRE].

[118] O. Stål and T. Stefaniak, *Constraining extended Higgs sectors with HiggsSignals*, *PoS* **EPS-HEP2013** (2013) 314 [arXiv:1310.4039] [iNSPIRE].

[119] ATLAS collaboration, *Search for heavy Higgs bosons with flavour-violating couplings in multi-lepton plus b-jets final states in pp collisions at 13 TeV with the ATLAS detector*, *JHEP* **12** (2023) 081 [arXiv:2307.14759] [iNSPIRE].

[120] CMS collaboration, *Search for an explanation to the muon anomalous magnetic moment through the non-resonant production of two additional Higgs bosons*, CMS-PAS-SUS-23-007 (2023) [iNSPIRE].

[121] ATLAS collaboration, *Search for the direct production of charginos and neutralinos in final states with tau leptons in $\sqrt{s} = 13$ TeV pp collisions with the ATLAS detector*, ATLAS-CONF-2022-042 (2022) [iNSPIRE].

[122] S. Iguro, T. Kitahara, M.S. Lang and M. Takeuchi, *Current status of the muon g-2 interpretations within two-Higgs-doublet models*, *Phys. Rev. D* **108** (2023) 115012 [arXiv:2304.09887] [iNSPIRE].

[123] M.E. Peskin and T. Takeuchi, *A new constraint on a strongly interacting Higgs sector*, *Phys. Rev. Lett.* **65** (1990) 964 [iNSPIRE].

[124] M.E. Peskin and T. Takeuchi, *Estimation of oblique electroweak corrections*, *Phys. Rev. D* **46** (1992) 381 [iNSPIRE].

[125] CDF collaboration, *High-precision measurement of the W boson mass with the CDF II detector*, *Science* **376** (2022) 170 [iNSPIRE].

[126] ALEPH et al. collaborations, *Electroweak Measurements in Electron-Positron Collisions at W-Boson-Pair Energies at LEP*, *Phys. Rept.* **532** (2013) 119 [arXiv:1302.3415] [iNSPIRE].

[127] D0 collaboration, *Measurement of the W Boson Mass with the D0 Detector*, *Phys. Rev. Lett.* **108** (2012) 151804 [arXiv:1203.0293] [iNSPIRE].

[128] LHCb collaboration, *Measurement of the W boson mass*, *JHEP* **01** (2022) 036 [arXiv:2109.01113] [iNSPIRE].

[129] ATLAS collaboration, *Measurement of the W-boson mass and width with the ATLAS detector using proton-proton collisions at $\sqrt{s} = 7$ TeV*, arXiv:2403.15085 [iNSPIRE].

[130] J. Bendavid, *High-precision measurement of the W boson mass at CMS*, LHC seminar [https://cds.cern.ch/record/2910496?ln=en].

[131] LHC-TeV MW Working Group collaboration, *Compatibility and combination of world W-boson mass measurements*, *Eur. Phys. J. C* **84** (2024) 451 [arXiv:2308.09417] [iNSPIRE].

[132] C.-T. Lu, L. Wu, Y. Wu and B. Zhu, *Electroweak precision fit and new physics in light of the W boson mass*, *Phys. Rev. D* **106** (2022) 035034 [arXiv:2204.03796] [iNSPIRE].

[133] D. Eriksson, J. Rathsman and O. Stål, *2HDMC: Two-Higgs-Doublet Model Calculator Physics and Manual*, *Comput. Phys. Commun.* **181** (2010) 189 [arXiv:0902.0851] [iNSPIRE].

[134] W. Grimus, L. Lavoura, O.M. Ogreid and P. Osland, *A precision constraint on multi-Higgs-doublet models*, *J. Phys. G* **35** (2008) 075001 [arXiv:0711.4022] [iNSPIRE].

[135] W. Grimus, L. Lavoura, O.M. Ogreid and P. Osland, *The oblique parameters in multi-Higgs-doublet models*, *Nucl. Phys. B* **801** (2008) 81 [arXiv:0802.4353] [iNSPIRE].

[136] Muon g-2 collaboration, *Measurement of the Positive Muon Anomalous Magnetic Moment to 0.20 ppm*, *Phys. Rev. Lett.* **131** (2023) 161802 [arXiv:2308.06230] [iNSPIRE].

[137] MUON G-2 collaboration, *Measurement of the Positive Muon Anomalous Magnetic Moment to 0.46 ppm*, *Phys. Rev. Lett.* **126** (2021) 141801 [arXiv:2104.03281] [INSPIRE].

[138] T. Aoyama et al., *The anomalous magnetic moment of the muon in the Standard Model*, *Phys. Rept.* **887** (2020) 1 [arXiv:2006.04822] [INSPIRE].

[139] M. Davier, A. Hoecker, B. Malaescu and Z. Zhang, *Reevaluation of the hadronic vacuum polarisation contributions to the Standard Model predictions of the muon $g-2$ and $\alpha(m_Z^2)$ using newest hadronic cross-section data*, *Eur. Phys. J. C* **77** (2017) 827 [arXiv:1706.09436] [INSPIRE].

[140] A. Keshavarzi, D. Nomura and T. Teubner, *Muon $g-2$ and $\alpha(M_Z^2)$: a new data-based analysis*, *Phys. Rev. D* **97** (2018) 114025 [arXiv:1802.02995] [INSPIRE].

[141] G. Colangelo, M. Hoferichter and P. Stoffer, *Two-pion contribution to hadronic vacuum polarization*, *JHEP* **02** (2019) 006 [arXiv:1810.00007] [INSPIRE].

[142] M. Hoferichter, B.-L. Hoid and B. Kubis, *Three-pion contribution to hadronic vacuum polarization*, *JHEP* **08** (2019) 137 [arXiv:1907.01556] [INSPIRE].

[143] M. Davier, A. Hoecker, B. Malaescu and Z. Zhang, *A new evaluation of the hadronic vacuum polarisation contributions to the muon anomalous magnetic moment and to $\boldsymbol{\alpha}(m_Z^2)$*, *Eur. Phys. J. C* **80** (2020) 241 [*Erratum ibid.* **80** (2020) 410] [arXiv:1908.00921] [INSPIRE].

[144] A. Keshavarzi, D. Nomura and T. Teubner, *$g-2$ of charged leptons, $\alpha(M_Z^2)$, and the hyperfine splitting of muonium*, *Phys. Rev. D* **101** (2020) 014029 [arXiv:1911.00367] [INSPIRE].

[145] A. Kurz, T. Liu, P. Marquard and M. Steinhauser, *Hadronic contribution to the muon anomalous magnetic moment to next-to-next-to-leading order*, *Phys. Lett. B* **734** (2014) 144 [arXiv:1403.6400] [INSPIRE].

[146] K. Melnikov and A. Vainshtein, *Hadronic light-by-light scattering contribution to the muon anomalous magnetic moment revisited*, *Phys. Rev. D* **70** (2004) 113006 [hep-ph/0312226] [INSPIRE].

[147] P. Masjuan and P. Sánchez-Puertas, *Pseudoscalar-pole contribution to the $(g_\mu - 2)$: a rational approach*, *Phys. Rev. D* **95** (2017) 054026 [arXiv:1701.05829] [INSPIRE].

[148] G. Colangelo, M. Hoferichter, M. Procura and P. Stoffer, *Dispersion relation for hadronic light-by-light scattering: two-pion contributions*, *JHEP* **04** (2017) 161 [arXiv:1702.07347] [INSPIRE].

[149] M. Hoferichter et al., *Dispersion relation for hadronic light-by-light scattering: pion pole*, *JHEP* **10** (2018) 141 [arXiv:1808.04823] [INSPIRE].

[150] A. Gérardin, H.B. Meyer and A. Nyffeler, *Lattice calculation of the pion transition form factor with $N_f = 2 + 1$ Wilson quarks*, *Phys. Rev. D* **100** (2019) 034520 [arXiv:1903.09471] [INSPIRE].

[151] J. Bijnens, N. Hermansson-Truedsson and A. Rodríguez-Sánchez, *Short-distance constraints for the HLbL contribution to the muon anomalous magnetic moment*, *Phys. Lett. B* **798** (2019) 134994 [arXiv:1908.03331] [INSPIRE].

[152] G. Colangelo et al., *Longitudinal short-distance constraints for the hadronic light-by-light contribution to $(g-2)_\mu$ with large-N_c Regge models*, *JHEP* **03** (2020) 101 [arXiv:1910.13432] [INSPIRE].

[153] G. Colangelo et al., *Remarks on higher-order hadronic corrections to the muon $g-2$*, *Phys. Lett. B* **735** (2014) 90 [arXiv:1403.7512] [INSPIRE].

[154] T. Blum et al., *Hadronic Light-by-Light Scattering Contribution to the Muon Anomalous Magnetic Moment from Lattice QCD*, *Phys. Rev. Lett.* **124** (2020) 132002 [`arXiv:1911.08123`] [InSPIRE].

[155] T. Aoyama, M. Hayakawa, T. Kinoshita and M. Nio, *Complete Tenth-Order QED Contribution to the Muon g-2*, *Phys. Rev. Lett.* **109** (2012) 111808 [`arXiv:1205.5370`] [InSPIRE].

[156] T. Aoyama, T. Kinoshita and M. Nio, *Theory of the Anomalous Magnetic Moment of the Electron*, *Atoms* **7** (2019) 28 [InSPIRE].

[157] A. Czarnecki, W.J. Marciano and A. Vainshtein, *Refinements in electroweak contributions to the muon anomalous magnetic moment*, *Phys. Rev. D* **67** (2003) 073006 [*Erratum ibid.* **73** (2006) 119901] [`hep-ph/0212229`] [InSPIRE].

[158] C. Gnendiger, D. Stöckinger and H. Stöckinger-Kim, *The electroweak contributions to $(g-2)_\mu$ after the Higgs boson mass measurement*, *Phys. Rev. D* **88** (2013) 053005 [`arXiv:1306.5546`] [InSPIRE].

[159] S. Borsanyi et al., *Leading hadronic contribution to the muon magnetic moment from lattice QCD*, *Nature* **593** (2021) 51 [`arXiv:2002.12347`] [InSPIRE].

[160] A. Boccaletti et al., *High precision calculation of the hadronic vacuum polarisation contribution to the muon anomaly*, `arXiv:2407.10913` [InSPIRE].

[161] M. Cè et al., *Window observable for the hadronic vacuum polarization contribution to the muon g-2 from lattice QCD*, *Phys. Rev. D* **106** (2022) 114502 [`arXiv:2206.06582`] [InSPIRE].

[162] EXTENDED TWISTED MASS collaboration, *Lattice calculation of the short and intermediate time-distance hadronic vacuum polarization contributions to the muon magnetic moment using twisted-mass fermions*, *Phys. Rev. D* **107** (2023) 074506 [`arXiv:2206.15084`] [InSPIRE].

[163] RBC and UKQCD collaborations, *Update of Euclidean windows of the hadronic vacuum polarization*, *Phys. Rev. D* **108** (2023) 054507 [`arXiv:2301.08696`] [InSPIRE].

[164] FERMILAB LATTICE et al. collaborations, *Light-quark connected intermediate-window contributions to the muon g-2 hadronic vacuum polarization from lattice QCD*, *Phys. Rev. D* **107** (2023) 114514 [`arXiv:2301.08274`] [InSPIRE].

[165] RBC and UKQCD collaborations, *Calculation of the hadronic vacuum polarization contribution to the muon anomalous magnetic moment*, *Phys. Rev. Lett.* **121** (2018) 022003 [`arXiv:1801.07224`] [InSPIRE].

[166] CMD-3 collaboration, *Measurement of the $e^+e^- \to \pi + \pi$- cross section from threshold to 1.2 GeV with the CMD-3 detector*, *Phys. Rev. D* **109** (2024) 112002 [`arXiv:2302.08834`] [InSPIRE].

[167] BABAR collaboration, *Precise Measurement of the $e^+e^- \to \pi^+\pi^-(\gamma)$ Cross Section with the Initial-State Radiation Method at BABAR*, *Phys. Rev. D* **86** (2012) 032013 [`arXiv:1205.2228`] [InSPIRE].

[168] KLOE-2 collaboration, *Combination of KLOE $\sigma\left(e^+e^- \to \pi^+\pi^-\gamma(\gamma)\right)$ measurements and determination of $a_\mu^{\pi^+\pi^-}$ in the energy range $0.10 < s < 0.95\,GeV^2$*, *JHEP* **03** (2018) 173 [`arXiv:1711.03085`] [InSPIRE].

[169] P. Masjuan, A. Miranda and P. Roig, *τ data-driven evaluation of Euclidean windows for the hadronic vacuum polarization*, *Phys. Lett. B* **850** (2024) 138492 [`arXiv:2305.20005`] [InSPIRE].

[170] M. Davier et al., *Tensions in $e^+e^- \to \pi^+\pi^-(\gamma)$ measurements: the new landscape of data-driven hadronic vacuum polarization predictions for the muon $g-2$, Eur. Phys. J. C* **84** (2024) 721 [arXiv:2312.02053] [INSPIRE].

[171] GAMBIT FLAVOUR WORKGROUP collaboration, *FlavBit: A GAMBIT module for computing flavour observables and likelihoods, Eur. Phys. J. C* **77** (2017) 786 [arXiv:1705.07933] [INSPIRE].

[172] GAMBIT MODELS WORKGROUP collaboration, *SpecBit, DecayBit and PrecisionBit: GAMBIT modules for computing mass spectra, particle decay rates and precision observables, Eur. Phys. J. C* **78** (2018) 22 [arXiv:1705.07936] [INSPIRE].

[173] GAMBIT collaboration, *ColliderBit: a GAMBIT module for the calculation of high-energy collider observables and likelihoods, Eur. Phys. J. C* **77** (2017) 795 [arXiv:1705.07919] [INSPIRE].

[174] S. Neshatpour and F. Mahmoudi, *Flavour Physics with SuperIso, PoS* **TOOLS2020** (2021) 036 [arXiv:2105.03428] [INSPIRE].

[175] GAMBIT collaboration, *Comparison of statistical sampling methods with ScannerBit, the GAMBIT scanning module, Eur. Phys. J. C* **77** (2017) 761 [arXiv:1705.07959] [INSPIRE].

[176] P. Scott, *Pippi-painless parsing, post-processing and plotting of posterior and likelihood samples, Eur. Phys. J. Plus* **127** (2012) 138 [arXiv:1206.2245] [INSPIRE].

[177] A. Greljo, J. Salko, A. Smolkovič and P. Stangl, *Rare b decays meet high-mass Drell-Yan, JHEP* **05** (2023) 087 [arXiv:2212.10497] [INSPIRE].

[178] ATLAS collaboration, *Search for a new scalar resonance in flavour-changing neutral-current top-quark decays $t \to qX$ $(q = u, c)$, with $X \to b\bar{b}$, in proton-proton collisions at $\sqrt{s} = 13$ TeV with the ATLAS detector, JHEP* **07** (2023) 199 [arXiv:2301.03902] [INSPIRE].

[179] ATLAS collaboration, *Snowmass White Paper Contribution: Physics with the Phase-2 ATLAS and CMS Detectors*, ATL-PHYS-PUB-2022-018 (2022) [INSPIRE].

[180] D.M. Asner et al., *ILC Higgs White Paper*, in the proceedings of the *Snowmass 2013: Snowmass on the Mississippi*, Minneapolis, U.S.A., July 29 – August 06 (2013) [arXiv:1310.0763] [INSPIRE].

[181] BELLE-II collaboration, *The Belle II Physics Book, PTEP* **2019** (2019) 123C01 [*Erratum ibid.* **2020** (2020) 029201] [arXiv:1808.10567] [INSPIRE].

[182] S.S. Wilks, *The Large-Sample Distribution of the Likelihood Ratio for Testing Composite Hypotheses, Annals Math. Statist.* **9** (1938) 60 [INSPIRE].

[183] T. Zheng et al., *Analysis of $B_c \to \tau\nu_\tau$ at CEPC, Chin. Phys. C* **45** (2021) 023001 [arXiv:2007.08234] [INSPIRE].

[184] Y. Amhis et al., *Prospects for $B_c^+ \to \tau^+\nu_\tau$ at FCC-ee, JHEP* **12** (2021) 133 [arXiv:2105.13330] [INSPIRE].

[185] X. Zuo et al., *Prospects for B_c^+ and $B^+ \to \tau^+\nu_\tau$ at FCC-ee, Eur. Phys. J. C* **84** (2024) 87 [arXiv:2305.02998] [INSPIRE].

[186] P. Athron et al., *Two-loop prediction of the anomalous magnetic moment of the muon in the Two-Higgs Doublet Model with GM2Calc 2, Eur. Phys. J. C* **82** (2022) 229 [arXiv:2110.13238] [INSPIRE].

[187] A. Cherchiglia, P. Kneschke, D. Stöckinger and H. Stöckinger-Kim, *The muon magnetic moment in the 2HDM: complete two-loop result, JHEP* **10** (2017) 242 [*Erratum ibid.* **10** (2021) 242] [arXiv:1607.06292] [INSPIRE].